THESIS

THE EFFECT OF PROJECTED SEA SURFACE TEMPERATURE CHANGE ON MJO ACTIVITY IN A WARMER CLIMATE

Submitted by

Amanda Francine Marie Bowden

Department of Atmospheric Science

In partial fulfillment of the requirements

For the Degree of Master of Science

Colorado State University

Fort Collins, Colorado

Fall 2023

Master's Committee:

Advisor: Eric D. Maloney

Jim Hurrell
Matthew Ross

ABSTRACT

THE EFFECT OF PROJECTED SEA SURFACE TEMPERATURE CHANGE ON MJO ACTIVITY IN A WARMER CLIMATE

The Madden Julian Oscillation (MJO) consists of a convective region that propagates eastward in the tropics on repeat every 30-90 days with peak amplitude during the Boreal Winter (November - March). Since the MJO modulates extreme weather such as tropical cyclones, atmospheric rivers, and monsoon variability, future MJO changes in a warmer climate have implications for prediction of extreme events. Understanding precipitation pattern changes in a changing climate is critical for freshwater resources and societal planning for oceanic regions. Decadal variability in the climate system causes patterns of sea surface temperature (SST) change in the tropical Pacific and associated precipitation, humidity, and wind pattern changes to vary from one decade to the next. MJO changes are strongly dependent on the pattern of SST change, and so understanding uncertainty in MJO change in future decades in the context of this decadal variability is the primary motivation for this investigation. Since climate models contain climate variability on decadal timescales, different initial conditions across ensemble members can result in diverse projection outcomes in any given decade. This investigation examines the impact of projected SST and moisture pattern changes over the 21st Century on MJO precipitation and zonal wind (850 mb) amplitude changes using 80 members with the SSP370 radiative forcing scenario from the Community Earth System Model 2 (CESM2) Large Ensemble. The projected SST and moisture pattern changes can be weighted more toward the central or eastern equatorial Pacific in earlier parts of the 21st Century across ensemble members, although becomes strongly El Niño-like later in the century. Ensemble members with stronger MJO precipitation amplitude in a given period are characterized by stronger El Niño-like east Pacific warming, associated with a strengthened meridional moisture gradient. As interpreted through moisture mode theory, greater east Pacific warming supports a stronger MJO by enhancing propagation through a stronger meridional moisture gradient, and enhancing MJO amplitude through a stronger vertical moisture gradient. The investigation supports the hypothesis that projected SST and moisture pattern changes influence

MJO activity, and also highlights the importance of understanding decadal climate variability for interpreting changes in water resources of oceanic regions.

ACKNOWLEDGMENTS

I would like to thank my advisor, Dr. Eric Maloney, for allowing me the golden opportunity to do my Master in Atmospheric Science at Colorado State University (CSU). He has been a role model for my coding and advice on my data analysis. I would like to thank my committee members at CSU, Jim Hurrell and Matt Ross for their help and suggestions for my research. I would like to thank everyone in the Maloney Research Group and the ATS West building for being great conversationalist of expanding my research and teaching new methods and knowledge about tropical meteorology to me. I would like to thank Carl Schreck and Jared Rennie for helping with the kf (zonal wavenumber-frequency) filter from ncl to python version, which is used to do spatial analysis for the MJO. I would like to thank my past mentors: Dr. John Knox (Univeristy of Georgia), Dr. Jennifer Collins (University of South Florida), Genevieve Miller (National Weather Service (NWS) Weather Forecasting Office (WFO) Guam), and Brandon Adylett (NWS WFO Guam) for their guidance during summer internship and research experiences. I would like to thank the CSU faculty and staff for their amazing work to take car of behind the scenes work for the department and myself. I would love to give an extra shout-out to Sarah Tisdale, who has been an amazing, kind friend and a great person to talk about anything with for me. I would like to thank the CSU ATS graduate students as well. I would like to thank my friends and family for supporting me in undergraduate and graduate school. I would love to give an extra shout-out to several of my best friends: Blake Checkoway (Texas Tech), Emily Luschen (University of Oklahoma), Kyle Brooks (University of Georgia), Jeremy Lewan (Rutgers University), Jasmine Keeler, Taylor Stephens, Rebecca Harvey, Emily Wolfe, Donna Mandujano, Peyton Lewis, Haley Stuckey (University of Georgia), and Parker Henry (Virginia Tech). These best friends have been an absolute rock in my life, and I could not have been as great without their never-ending support and their love for me. This work has been supported by the National Science Foundation at Colorado State University under the cooperative agreement No. AGS-1841754. The dataset used is the Community Earth System Model 2 (CESM2) and is downloaded from the National Center for Atmospheric Research (NCAR) website. This work is an adaptation of CSU Research Experience from Undergraduates (REU), but using the CESM2.

DEDICATION

To Sonikku, Maw/Maw, Mother, and Father

TABLE OF CONTENTS

ABSTRACT ii

ACKNOWLEDGMENTS iv

DEDICATION v

LIST OF FIGURES viii

Chapter 1. Introduction 1

1.1 The Madden Julian Oscillation 1

1.1.1 MJO Formation 1

1.1.2 MJO Maintenance 4

1.1.3 MJO Propagation 4

1.1.4 MJO Impacts and Influences 6

1.1.5 MJO in a Warmer Climate 7

1.2 Sea Surface Temperatures (SSTs) influence on the MJO 8

1.3 Oceanic Regions and their Pacific Islands 8

1.4 The Community Earth System Model (CESM) 10

1.5 Chapter Review 11

Chapter 2. The Effect of Projected Sea Surface Temperatures on Mean Precipitation Change . . . 13

2.1 Chapter 2 Prelude 13

2.2 Data and Methodology 13

2.3 Results and Discussion 15

2.3.1 Preferential Concentration of SST warming and Precipitation Formation 15

2.3.2 Objective Measures of SST Pattern Changes in the Equatorial Pacific 20

2.3.3 Precipitation Pattern Changes of Pacific Islands and Oceanic Regions 21

2.4 Conclusion 24

Chapter 3. MJO Activity in a Future Warmer Climate 26

3.1 Chapter 3 Prelude 26

3.2 Data and Methodology 26

3.3 Results and Discussion 27
3.3.1 MJO Activity Change in a Future Climate 27
3.3.2 SST Pattern Changes for the Strongest MJO Amplitude Changes 30
3.3.3 MJO Activity versus SST in Oceanic Regions 31
3.4 Conclusion 33

Chapter 4. Vertical Moisture effect on MJO Activity in a Future Warmer Climate 34
4.1 Chapter 4 Prelude 34
4.2 Data and Methodology 34
4.3 Results and Discussion 35
4.3.1 Precipitable Water in a Future Climate 35
4.3.2 MJO Activity Plus and Minus of Precipitable Water 36
4.3.3 Vertical Moisture Profile influencing MJO Activity 39
4.4 Conclusion 42

Chapter 5. Conclusion 44

References 47

Appendix A. Frequency-Wavenumber MJO Amplitude Tool 58

LIST OF FIGURES

Fig. 1.1 Diagram of the MJO Convective and Suppressed Phase from NOAA 3

Fig. 1.2 Multiscale tropical (and mesoscale) convective systems vertical structures of cloud formation associated with moisture and temperature referenced from Kiladis et al. (2009); Jiang et al. (2020) 5

Fig. 1.3 Map of Oceanic Regions with interest are Polynesia, Micronesia, and Melanesia based on the United Nations geoscheme M49 coding classification devised by the United Nations Statistics Division. 9

Fig. 2.1 Map of Oceanic Regions of interest are Central Polynesia, Micronesia, and Melanesia based on the United Nations geoscheme M49 coding classification devised by the United Nations Statistics Division 15

Fig. 2.2 Mean Sea Surface Temperature (SSTs) and Precipitation during the historical baseline period of 1985 to 2005 16

Fig. 2.3 Change of 2021-2040 Sea Surface Temperatures (SSTs) and Precipitation Relative to 1985 to 2005 for one ensemble member out of all 80 members that exhibit more east Pacific (top), central Pacific (middle), and west Pacific (bottom) warming 17

Fig. 2.4 Change of 2041-2060 Sea Surface Temperatures (SSTs) and Precipitation Relative to 1985 to 2005 for one ensemble member out of all 80 members that exhibit more preferential warming pattern to the east Pacific (top), central Pacific (middle), and west Pacific (bottom) 18

Fig. 2.5 Change of 2061-2080 Sea Surface Temperatures (SSTs) and Precipitation Relative to 1985 to 2005 for one ensemble member out of all 80 members that exhibit more preferential warming pattern to the east Pacific (top), central Pacific (middle), and west Pacific (bottom) 19

Fig. 2.6 Pattern Change of Sea Surface Temperatures (SSTs) in Niño3.4 and East-West Relative to 1985 to 2005 in the Pacific 21

Fig. 2.7 10-yr running mean of rainfall rate relative to 1985 to 2005 for Pacific Islands a) Guam, b) Samoa, c) Kirbati, d) Galapagos Islands, e) Solomon, and f) Palau 22

Fig. 2.8 10-yr running mean of rainfall rate change relative to 1985 to 2005 for Oceanic Regions a) Central Polynesia, b) Micronesia, and c) Melanesia 23

Fig. 3.1 Top row: Ensemble mean MJO precipitation and 850 mb zonal wind standard deviation for the 1985-2005 period. Bottom rows, the percentage change in MJO Activity relative to 1985 to 2005 based on 20-yr decadal periods. 28

Fig. 3.2 MJO amplitude change versus Niño3.4 SST Change. Precipitation and 850 mb zonal wind amplitude change across the entire Tropics relative to 1985 to 2005 is shown for two 20-year periods 30

Fig. 3.3 Difference in SST change for the ensemble members with top 33% of MJO amplitude change (MJO Plus) minus the bottom 33% of MJO amplitude change (MJO Minus). Precipitation and zonal wind amplitude changes are analyzed for different 20 yr periods 31

Fig. 3.4 Relationship between Niño3.4 Sea Surface Temperatures Change and MJO amplitude change for three oceanic regions: Central Polynesia, Micronesia, and Melanesia for 2041-2060. Precipitation and zonal wind amplitude changes are analyzed. Correlations that are shaded are statistically significant. 32

Fig. 3.5 Same as Figure 3.4, but for 2081-2100. 33

Fig. 4.1 Historical (1985-2005) precipitable water distribution (top panel) and its percentage change relative to the historical period (bottom panels) 36

Fig. 4.2 Same as Figure 3.3, except for TMQ 37

Fig. 4.3 Same as Figure 4.2, except for TMQ gradient 38

Fig. 4.4 Relationship between MJO amplitude change averaged over the entire tropics and Central Pacific TMQ meridional gradient change for precipitation and 850 mb zonal Wind relative to 1985 to 2005 for two 20-yr periods 39

Fig. 4.5 Change of tropical Pacific vertical specific humidity profile at the Equatorial Pacific associated with the members having the top 33% minus bottom 33% of MJO amplitude changes based on precipitation and 850 mb zonal wind. Changes are defined relative to 1985 to 2005 40

Fig. 4.6 Relationship between MJO precipitation and wind amplitude change averaged over the entire tropics and lower tropospheric specific humidity change at the Equatorial Pacific relative to 1985 to 2005 for two 20-yr periods 41

Fig. 4.7 Relationship between MJO precipitation and wind amplitude change averaged over the entire tropics and vertical specific humidity gradient change at the Equatorial Pacific relative to 1985 to 2005 for two 20-yr periods 42

CHAPTER 1

INTRODUCTION

Tropical Pacific islands and coastlines are vulnerable to sea level rise, intensified tropical cyclones, droughts, and other effects of climate change because of their smaller land mass sizes and large indigenous population. These indigenous communities do not have access to resources to recover as quickly from natural disasters as other core and semi-periphery countries. SST warming can adversely affect these oceanic regions and coastlines by increasing the likelihood of extreme weather, and through other factors such as sea level rise. Preferential SST warming toward the central and eastern Pacific region can promote increased precipitation anomalies for those regions, but promote more drought-like conditions for the western Pacific. These effects are reversed when there is preferential SST warming toward the western Pacific domain, which means more concentration of SST in that specific region.

This investigation evaluates the impact of projected SST changes over the 21st Century from the SSP370 forcing scenario on precipitation and winds in the tropics using ensemble members from the Community Earth System Model (CESM2; Rodgers et al. 2021). In addition to the effect on mean precipitation and winds, this investigation analyzes the effect of SST pattern change on tropical variability. In particular, this investigation is interested in how the pattern of SST change in a given period (e.g. 20-years) can affect propagation and maintenance of the Madden Julian Oscillation (MJO; Madden and Julian 1971), and seeks to understand the underlying reasons for the changes through moisture mode theory.

It is found that changes in MJO activity in a future climate are dependent on horizontal and vertical basic state moisture gradient changes, which are associated with SST pattern changes. Understanding uncertainties in projections for the tropics can aid adaptation and mitigation strategies to help combat the intensified effects and hazards of mean state global precipitation and circulation changes, and also changes to modes of variability such as the MJO.

1.1 THE MADDEN JULIAN OSCILLATION

1.1.1 MJO FORMATION

The MJO is an intraseasonal mode of tropical climate variability characterized by clusters of convective storms that propagate eastward. These clusters are accompanied by fluctuations of precipitation, clouds, winds, and pressure that span the global tropics. The MJO was discovered by Madden and Julian (1971) using power spectrum analysis on zonal winds at multiple pressure levels from different

station soundings (Bingham et al. 1967). The Madden and Julian (1971) investigation noted a signal concentrated in the 40-50 day period band. However, recent literature suggests that the MJO signal is found on a broader frequency band around 30-90 days based on more comprehensive wavenumber-frequency spectral analysis and more comprehensive datasets (Wheeler and Kiladis 1999; Raymond and Fuchs 2009; Maloney and Xie 2013). Further investigation showed that the MJO has a global signal that spans the tropics, propagating eastward with an out of phase relationship between upper and lower tropospheric horizontal winds (Madden and Julian 1972; Hayashi and Itoh 2017; Jiang et al. 2020).

The MJO is the strongest during boreal winter (December - February), and weakest during boreal summer (June to August) (Madden and Julian 1994; Wheeler and Kiladis 1999). The MJO cyclically transitions from an active to a suppressed convective phase. The convective phase is associated with enhanced rainfall and rising motion with winds converging in the lower troposphere and diverging in the upper troposphere. The convective phase of the MJO is associated with a thermodynamic balance between adiabatic cooling caused by upward motion and diabatic heating (Sobel and Maloney 2012, 2013). The convective phases can be enhanced by cloud-radiative and wind-evaporative feedbacks (Maloney 2009). In contrast, the suppressed phase is associated with subdued rainfall and associated sinking motion with lower tropospheric divergence and upper tropospheric convergence (Wheeler and Hendon 2004; Gottschalck 2014) seen in Figure 1.1.

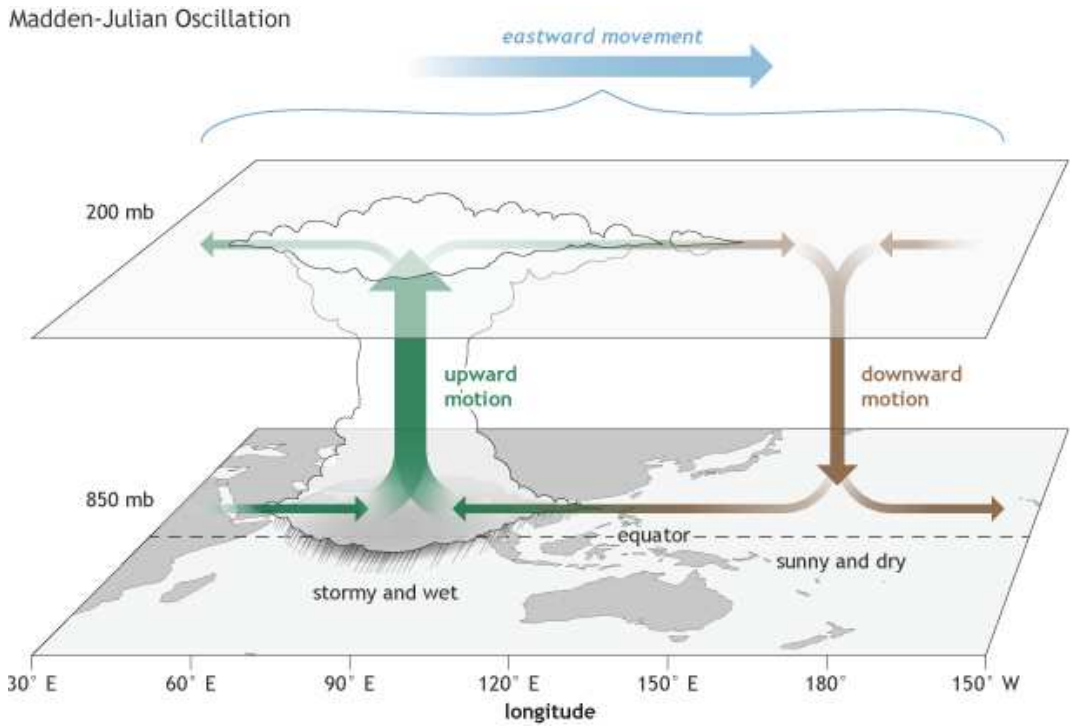

FIG. 1.1. Diagram of the MJO Convective and Suppressed Phase from NOAA

The MJO originates over the Indian Ocean before propagating eastward through the Indo-Pacific warm pool, which is a major heat and moisture source for the global circulation, and a region of high annual precipitation (Madden and Julian 1994; Jiang et al. 2020). The MJO propagates eastward at around 5 m/s in the Indo-Pacific warm pool, but eventually speed up in other locations in the tropics. MJO activity can be broken into 8 zonal phases that describe the spatial evolution of its precipitation and wind signal based on the geographical location of precipitation anomalies and wind convergence in the tropics (Madden and Julian 1971; Wheeler and Hendon 2004; Jiang et al. 2020). Phase 1 is associated with convective initiation over the western Indian Ocean. In Phases 2 and 3, the system moves slowly eastward across the Indian Ocean, with suppressed convection in the West Pacific. Phases 4 and 5 indicates the enhanced convection moving through the Maritime Continent (MC). Lastly, in Phases 6 through 8, the convective core propagates through the western Pacific until weakening occurs in the central Pacific (Wheeler and Hendon 2004; Jiang et al. 2020). Even though the MJO weakens in the central Pacific, a warmer climate might produce more sustained propagation into the eastern Pacific (Jiang et al. 2020).

1.1.2 MJO MAINTENANCE

A comprehensive explanation for the MJO remains elusive, although a consensus has been emerging that processes regulating the moisture field are important for understanding MJO dynamics. Theories about the MJO formation and dynamics that have been proposed range from moisture convective coupling, cloud radiative feedback, and wave interaction with planetary to mesoscale systems (Jiang et al. 2020). This investigation uses moisture mode theory to interpret MJO changes under a warming climate. The first indication that moisture is a key aspect to MJO dynamics was an analysis of mixing ratio variability as a function of MJO phase in sounding data (Madden and Julian 1972). More recently, the importance of moisture to MJO dynamics has matured into a body of theory called moisture mode theory (Sobel and Maloney 2012, 2013). Under this body of theory, the tropical atmosphere is assumed to be in a condition of weak temperature gradients (WTG), which suggest little to no horizontal temperature differences above the boundary layer in the Indo-Pacific warm pool region. While waves are assumed to be not of first order importance to the dynamics of the MJO due to horizontal temperature variations being neglected, the humidity anomalies are of first-order importance because of the strong link between convection and vertically integrated water vapor (Neelin and Held 1987; Sobel and Bretherton 2000; Hayashi and Itoh 2017). Moisture mode theory claims that free tropospheric moisture perturbations and the processes that help maintain them, such as surface flux feedbacks and destabilization by cloud radiative feedbacks, help to support MJO related precipitation anomalies and eastward propagation (Sobel and Maloney 2012, 2013). In a moisture mode, processes that increase moisture anomalies support disturbance growth, and processes that support a moisture tendency to the east of convection such as horizontal moisture advection support eastward propagation. A prognostic humidity equation underpins moisture mode models of the MJO that describe these dynamics (Sobel and Maloney 2012). Conditions that support convection under moisture mode theory include strong moistening in the region of low-level easterlies to the east of convection, enhanced surface wind evaporation, cloud radiative feedbacks, and moist static instability tied to high SSTs (Sobel and Maloney 2013). These processes are discussed in more detail below.

1.1.3 MJO PROPAGATION

Eastward MJO propagation is supported by moistening processes to the east of convection, including horizontal moisture advection, warm sea surface temperatures, boundary layer convergence, low-level heating by shallow clouds, increasing enhanced free tropospheric moisture anomalies, and

a Kelvin wave-like wind response (Waliser 1996; Kiladis et al. 2009; Jiang et al. 2020). Shallow cumulus clouds and associated lower tropospheric vertical motion help moisten the troposphere to the east of MJO convection and make the environment more suitable for convection (Waliser 1996; Sobel and Bretherton 2000). In contrast to the region east of the MJO convection, the region west of MJO convection is characterized by upper level tropospheric stratiform clouds and low-level westerly winds that amplify surface turbulent fluxes associated with a Rossby wave-like response. While the vertical mass flux profile associated with stratiform clouds tend to dry the atmosphere, enhanced surface fluxes partially cancel this drying effect. Shallow circulation moistening to the east and stratiform heating to the west for MJO convection favors eastward propagation, thus supporting propagation under moisture mode theory (Waliser 1996; Sobel and Bretherton 2000; Kiladis et al. 2009; Maloney 2009; Jones and Carvalho 2011; Jiang et al. 2020). Some of these salient processes are summarized in Figure 1.2 (Kiladis et al. 2009; Raymond and Fuchs 2009; Hayashi and Itoh 2017).

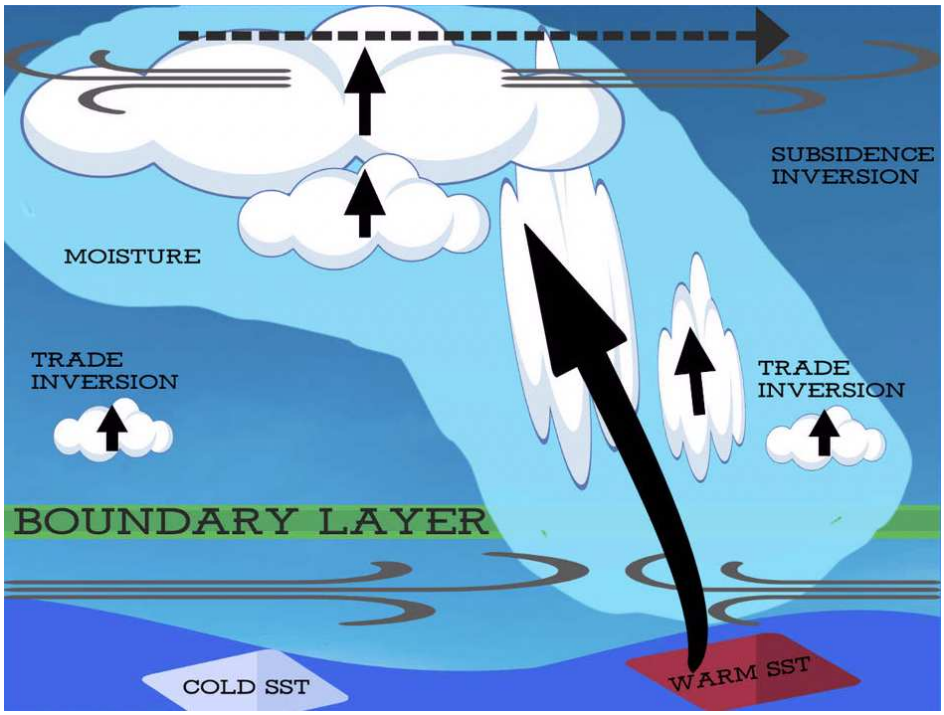

FIG. 1.2. Multiscale tropical (and mesoscale) convective systems vertical structures of cloud formation associated with moisture and temperature referenced from Kiladis et al. (2009); Jiang et al. (2020)

The dominant process for regulating moistening or drying the east/west of MJO convection is horizontal advection (Maloney 2009). Particularly important to this thesis is that meridional advection by the anomalous MJO wind acting on the mean moisture gradient is a dominant factor in moistening to

the east of MJO convection (Kim et al. 2017). The winter mean low level moisture pattern over the MC supports MJO propagation through horizontal moisture advection (Gonzalez and Jiang 2017). Interannual variability in the climate system can effect this horizontal advection moistening tendency to the east of MJO convection. The mean precipitable water distribution shifts eastward during El Niño events, reducing the background zonal and meridional moisture gradients and supporting transient dry precursors (DeMott et al. 2018). Both processes would inhibit eastward MJO propagation, suggesting a strong influence from climate variability on the basic state conditions that support MJO propagation. Overall, a stronger meridional moisture gradient supports MJO propagation through the tropics by enhancing horizontal moisture advection.

Other processes also support MJO eastward propagation. In regions of low-level easterlies to the east of MJO convection, frictional convergence in the equatorial boundary layer produces a narrow region of shallow, upward motion that supports a bottom-heavy convective profile to the east of maximum ascent, which helps to moisten the lower to mid-troposphere (Maloney and Hartmann 1998; Kiladis et al. 2005). The vertical moisture advection from the ascent helps with eastward propagation by growing moisture anomalies to the east of MJO convection (Adames and Wallace 2015).

The MC can limit MJO propagation through barrier effects and other factors, and was first hinted at by Madden and Julian (1971). The MC islands mountain topography acts as an orographic blockage disrupting formation of low-level convergence to the east of MJO convection. The islands can also disrupt the coupled Kelvin-Rossby wave structure of the MJO (Jiang et al. 2020). The MC has also been suggested to weaken convection by causing an abrupt end of the lower tropospheric moisture needed for convection formation and its propagation (Adames and Maloney 2021). The MC barrier effect is an interesting test case for understanding MJO dynamics and for interpreting the effect of climate change on the MJO. For instance, one study showed that models producing better MJO propagation through the MC have stronger meridional moisture gradients (Kang et al. 2021). This suggests that models with stronger meridional moisture gradients in a warmer climate produce more prominent eastward propagation. Overall, an increased meridional moisture gradient supports eastward MJO propagation.

1.1.4 MJO Impacts and Influences

MJO activity can help to enhance tropical systems by providing more moisture to the atmosphere that likely feeds extreme weather events such as extreme precipitation. The mean flow is intensified after the passage of the MJO convective region, thus affecting mesoscale to synoptic scale systems, and global systems through teleconnections (Madden and Julian 1994; Jiang et al. 2020). For example,

the MJO strongly modulates the intensity of atmospheric rivers (ARs), which transport moisture to remote areas and can cause flooding events, particularly on the west coast of North America (Zhou et al. 2021). Further, periods of low-level westerly winds, enhanced moisture, cyclonic flow, and reduced shear produced by the anomalous MJO circulation make conditions favorable for hurricane genesis (Maloney and Hartmann 2000). While MJO activity can modulate shorter timescale phenomena, the MJO can also interact with longer timescale global oscillations and circulations. The MJO is modulated by the Quasi-Biennial Oscillation (QBO), which is a tropical stratospheric interannual variability mode. MJO activity is enhanced for easterly QBO conditions, but suppressed by the westerly QBO (Huang et al. 2023). The MJO can also influence other oscillations such as North Atlantic Oscillation (NAO), especially through an El Niño Southern Oscillation (ENSO) background state dependency, the state of which can conversely help to modulate MJO strength during boreal winter. For instance, the MJO teleconnections is stronger with the NAO due to increased likelihood of positive NAO after MJO phases 1 through 5 in El Niño years (Lee et al. 2019; Jiang et al. 2020).

1.1.5 MJO IN A WARMER CLIMATE

MJO activity is highly sensitive to tropical SST change, and is expected to increase in intensity in a future warmer climate to first order due to stronger basic state vertical moisture gradients with warming (Maloney and Xie 2013; Bui and Maloney 2018; Kang et al. 2021). This increased moisture gradient makes moistening of the atmosphere by vertical advection more effective, supporting stronger MJO precipitation (Maloney et al. 2019). Models generally predict an increase in MJO precipitation amplitude and frequency of MJO events with warming based on a shorter temporal scale, especially in the MC (Jones and Carvalho 2011; Maloney and Xie 2013; Jiang et al. 2020; Adames and Maloney 2021). The response of MJO winds to warming is more complicated, with some models projecting weakening of MJO zonal wind amplitude, even with increased MJO precipitation variance (Bui and Maloney 2018; Jiang et al. 2020; Adames and Maloney 2021). These results are consistent with tropical WTG thermodynamic balance, which mandates that increases in the tropical static stability with warming are associated with a weaker circulation per unit diabatic heating (Hsiao et al. 2020). The MJO becoming stronger in a warmer environment could result in stronger enhanced and suppressed phases, which may cause its modulation of ARs and TCs to become stronger (Bui and Maloney 2018; Maloney and Hartmann 2000; Zhou et al. 2021). However, the weakening of MJO circulations per unit precipitation may complicate this (Bui and Maloney 2022). The intensification of climate change hazards by the MJO

could also affect vulnerable communities (Bui and Maloney 2018). More nuanced discussion on how the pattern of SST change affects MJO change in a warmer climate is contained below.

1.2 Sea Surface Temperatures (SSTs) influence on the MJO

Climate models show differences in future warming patterns across models, and on decadal timescales within individual models (Rugenstein et al. 2020; Bui et al. 2023). The pattern of SST change provides uncertainty in how the MJO will respond to a warmer climate. A study using an aquaplanet GCM forced by with a variety of SST warming patterns, but with the same global mean temperature change, was used to understand the MJO response to climate change (Maloney and Xie 2013). While a uniform warming pattern caused increases in MJO precipitation variance as expected, some SST warming patterns produced a decrease in MJO precipitation amplitude. For all cases, the ratio of MJO wind amplitude to precipitation amplitude decreased due to increases in tropical static stability with climate warming. The Maloney and Xie (2013) results signify that future MJO precipitation amplitude changes are highly linked to the SST warming pattern, and those precipitation variance changes can help predict MJO wind variance changes through WTG thermodynamic balance. Some investigations have also shown the MJO follows maxima in the meridional SST gradients, with the maximum amplitude off the equator (Raymond and Fuchs 2009). In general, horizontal SST gradients have been shown to increase convective activity (Tompkins 2001). Thus, even relatively modest SST gradient shift changes can affect large-scale organized convection, including the MJO (Trenberth et al. 1998). In the current climate, years with El Niño SST anomalies increase the mean meridional moisture gradient in the MC region and support MJO propagation through increased horizontal moisture advection (Kang et al. 2021). Takahashi et al. (2011) showed that climate model projections with more El Niño-like warming patterns tend to produce stronger MJO amplitude, with the opposite for those with more La Niña-like warming patterns. Thus, while warmer SSTs generally increase the vertical moisture gradient that supports a stronger MJO (Maloney 2009), there is also a pattern effect to warming on the MJO. This is what will be addressed in this study.

1.3 Oceanic Regions and their Pacific Islands

Pacific islands are vulnerable communities based on their geographical remoteness, high dependency on trade for livelihood, vulnerability to economic shocks, and highly susceptibility to climate change hazards. These climate change hazards include sea level rise, intensified tropical cyclones, prolonged droughts, heatwaves, and forest fires (Schroeder et al. 2012; Abraham et al. 2022). These

tropical islands are rich biodiversity hotspots with local native plants and vegetation, coral enriched oceans, and high fish population patterns (Abraham et al. 2022). The majority of Pacific islanders live within 5 km of the coast, putting them in high risk areas for extreme weather events impacts (Mycoo et al. 2022). Thus, small Pacific islands and their ecosystems are more vulnerable to climate change (Lefale 2010).

Hawaii and the U.S Affiliated Pacific Islands composed of Guam, Commonwealth of the Northern Mariana Islands, Republic of Palau, Marshall Islands, Federated States of Micronesia, and American Samoa seen in Figure 1.3 tend to be overlooked in research (Schroeder et al. 2012). Guam is a small island in the western Pacific where extreme rainfall and flooding can provide great impacts. One study analyzed extreme annual maximum precipitation on Guam using intensity-duration-frequency (IDF) curves. The results show extreme rainfall is highly dependent on extreme weather events, for instance, typhoons impact increased daily IDF curves by 3% for the island (Yeo et al. 2022).

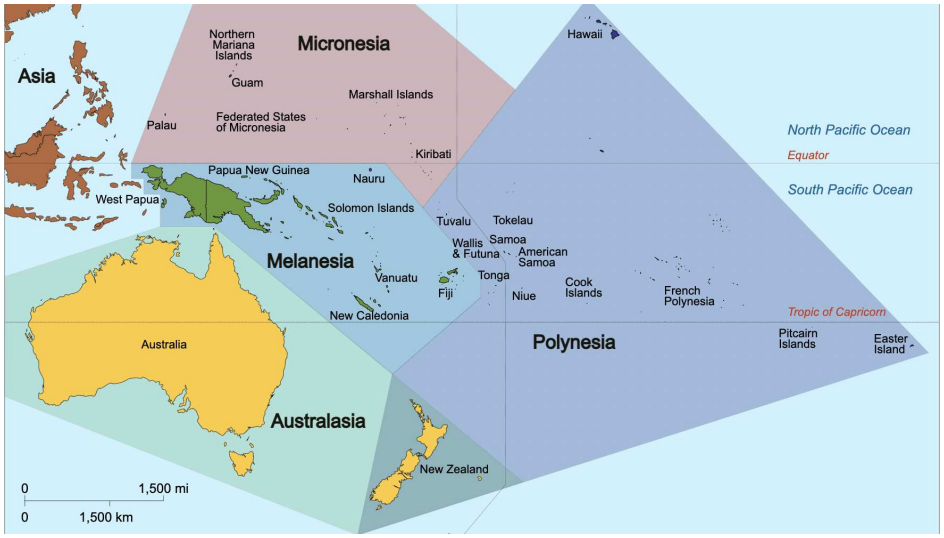

FIG. 1.3. Map of Oceanic Regions with interest are Polynesia, Micronesia, and Melanesia based on the United Nations geoscheme M49 coding classification devised by the United Nations Statistics Division.

El Niño-like SST variations can result in increased forest fires, drier conditions, altered fishing habits, prolonged droughts, flash floods associated with increased tropical cyclones, lowered sea level, colder ocean conditions, and food shortages for the western Pacific. In contrast, the eastern Pacific experiences more rainfall and reduced nutrient rich upwelling associated with weakening currents along the West Coast of the Americas (Schroeder et al. 2012). It is worth noting that mean state changes that look El Niño-like produce similar impacts on precipitation in the Pacific.

With the impacts of climate change, high confidence exists that vulnerability will increase for oceanic regions and their islands (Schroeder et al. 2012; Mycoo et al. 2022). The climate change impacts to islands are seen through SST warming, sea level rise, salinity increases to water supplies, biodiversity reduction, ocean acidification, coral bleaching, intensified storms, negative production of island agriculture, and drastic hydrological changes (Abraham et al. 2022). One study that evaluated Guam IDF curves from extreme rainfall patterns noted the need for better understanding to improve storm-water manager systems and improve hazard mitigation (Yeo et al. 2022).

Another study investigated Samoa's forecasting strategies for cloud types and tropical cyclones. The study calls for the need for better synthesis of contemporary western scientific methodologies of weather and climate with indigenous forecasting practices to help improve weather education, especially with climate change (Lefale 2010). Projections for the tropics can provide much needed support in the form of adaptation and mitigation strategies to help combat the intensified effects and hazards of global climate and circulation changes associated with mean state changes, and also changes to modes of variability such as MJO and ENSO (Mycoo et al. 2022).

1.4 The Community Earth System Model (CESM)

The usage of climate modeling can provide information on potential future climate and weather conditions under greenhouse gas warming scenarios. While Earth system models are simplified representations of the Earth system and their future climate projections are likely imperfect, models provide valuable information to the public, government, and other researchers that can be used to guide adaptation and mitigation strategies under a changing climate (Mycoo et al. 2022). Models produce an evolution of future temperature anomalies in response to increased CO_2 and other factors that have arisen since the rise of the industrial revolution, as well as natural forcing agents (Xie et al. 2010). Differences in the initial conditions in individual model ensemble members can produce a different evolution of climate variability and weather on decadal timescales. Projected climate states are highly sensitive to small differences in initial conditions, similar to the dependence in synoptic weather prediction (Lorenz 1963). Different initial ocean-atmosphere states can produce very different decadal SST patterns into the future, with implications for climate projections under global warming over the 21st Century (Abraham et al. 2022).

The Community Earth System Model (CESM) is a numerical model that includes atmospheric, ocean, ice, land surface, and carbon cycle components that can be used to simulate past climate or

can be used for climate projections (Hurrell et al. 2013). The CESM can be used to analyze projections on short term (e.g. weeks, years) and longer (e.g. decadal to century) time scales to assess global trends, global warming hiatus periods, and conduct statistical evaluation for specified meteorological, oceanic, and land surface components (Kay et al. 2015). The newest version, CESM2, has a grid resolution of 1.25° x 0.94° (Danabasoglu et al. 2020). CESM2 model improvements relative to the previous version involve a better historical simulation, and better representation of global oscillations, circulations, and teleconnection patterns (Rodgers et al. 2021). CESM2 models have also been shown to have better representation of the MJO compared to the CESM1 (Danabasoglu et al. 2020). Shared socioeconomic pathways (SSP) incorporate different assumptions about economic activity and mitigation and adaptation strategies to model Greenhouse gas (GHG) emissions (Riahi et al. 2017; Mycoo et al. 2022).

Climate model ensembles having different initial conditions allow each member to have a different future evolution of decadal climate variability. While future predictions of climate are more complicated with decadal variability in the climate system (Diffenbaugh and Barnes 2023), ensembles provide opportunities to characterize this uncertainty. Even though the CESM is useful, it still has limitations. For instance, modeling errors can cause potential biases in objective analysis of predictive climate patterns. One study shows that model mean state biases lead to errors of variability patterns that reduces the validity of future projections (Richter and Doi 2019). Models like the CESM2 have some biases with more warming toward the eastern Pacific than in the observed record. Most models haven't been able to replicate the recent La Niña-like warming trend in observations (Yang et al. 2018). Further, while the relatively coarse resolution model gives average spatial conditions over the grid box, which may not be truly reflective of reality and lead to inadequate representation of impacts of future climate change for islands (Mycoo et al. 2022).

1.5 Chapter Review

This thesis addresses the impact of SST pattern change on the amplitude of the MJO in a future warmer climate. It is motivated by previous studies that have shown that future changes to the MJO are highly sensitive to the pattern of SST change in the tropics (Maloney and Xie 2013).

This investigation is motivated by three main hypotheses: (1) The pattern of projected SST change directly influences mean precipitation and wind change in the Tropics. (2) The pattern of SST change strongly influences MJO behavior in a future warmer climate. An eastern Pacific warming pattern, whether a transient decadal pattern or a long-term trend, is expected to intensify the MJO. (3) Changes

to the mean vertical moisture gradient and horizontal surface temperature and moisture gradients can be used to understand how MJO activity is influenced by SST pattern changes.

In Section 2, the investigation discusses how SST pattern changes in the CESM2 LENS influence the mean precipitation change during different decadal periods. It then relates changes in SST warming patterns to mean precipitation change on individual tropical islands. In Section 3, the study analyzes how projected SST pattern changes in future decades influence MJO activity, including changes to the spatial distribution of MJO variance. In Section 4, the investigation evaluates how differing changes to the mean vertical and horizontal moisture gradients among ensemble members regulate MJO amplitude change. These differences in gradient relate to differing patterns of SST change among ensemble members. Conclusions follow in Section 5.

CHAPTER 2

THE EFFECT OF PROJECTED SEA SURFACE TEMPERATURES ON MEAN PRECIPITATION CHANGE

2.1 CHAPTER 2 PRELUDE

The investigation discusses how projected SST pattern changes relative to the historical period influence mean precipitation change. Simulations with preferential warming weighted more toward the eastern, central, or western Pacific are identified for 20-yr periods in the future. It takes a further step to quantify the relative warming of the east Pacific relative to west Pacific across ensemble members from earlier decades until the end of the 21st Century. Because climate models contain climate variability such as the Pacific Decadal Oscillation (PDO) and other global oscillations, each ensemble member can have diverse projection outcomes in a given decade (Waliser 1996; Trenberth et al. 1998). Implications of these SST pattern changes on mean precipitation change on different Pacific islands are analyzed.

In particular, this investigation analyzes projected SST and precipitation patterns in the CESM2 large ensemble under a relatively high-end forcing scenario, SSP370, associated with 7.0 $\frac{W}{m^2}$ of climate forcing at 2100. This investigation examines the mean change in the tropics, as well as the implications of decadal variability for mean precipitation on Pacific islands. The proposed investigation questions are (1) how uncertain are the patterns of SST change in the future due to decadal variability in Section 2.3.1, (2) to what extent does the pattern of projected SST change influence precipitation change in the Tropics in Section 2.3.2, and (3) what are the implications for precipitation on islands in the Pacific and oceanic regions in Section 2.3.3.

2.2 DATA AND METHODOLOGY

The model used is the CESM2 with the radiative forcing under SSP370, which is one of the highest forcing scenarios for CMIP6 (Riahi et al. 2017; Rodgers et al. 2021). The dataset analyzes changes in SST warming patterns and precipitation in 80 ensemble members from the CESM2 LENS. The base historical state to assess SST and precipitation changes into the future is the ensemble mean from 1985-2005:

$$X_{patternchanges} = X_{future} - \bar{X}_{1985\text{–}2005}, \tag{2.1}$$

This investigation evaluates the SST pattern change across different ensemble members. During a given 20-year period, SST and precipitation changes can be more weighted toward the eastern, central

or western Pacific due to decadal variability. This analysis of pattern change for the different ensemble members is a combination of subjective analysis using visual inspection, and objective analysis based on positive or negative rates of East versus West Pacific warming (Meehl and Washington 1996).

The degree of east Pacific warming relative to the west can be calculated by taking the difference of the SST change between east and west Pacific boxes, defined by 10-year running means for East (5°S - 5°N, 120°W - 90°W) and West (5°S - 5°N, 140°E - 170°E) boxes, consistent with Meehl and Washington (1996) and Trenberth (1997). Changes in the Niño3.4 (5°S - 5°N, 120°W - 170°W) timeseries giving a simple measure of east Pacific warming are provided for comparison.

Since Pacific tropical islands and adjacent oceanic regions are vulnerable communities to climate change impacts, this investigation takes a step further by analyzing the implication of SST pattern changes and their uncertainty for mean precipitation changes for Pacific islands (Lefale 2010; Mycoo et al. 2022; Yeo et al. 2022). The investigation uses multiple islands including Guam (13°N and 145°E), Samoa (13.5°S and 172°W), Kirbati (1.5°N and 157°W), Galapagos Islands (-1°S and 90°W), Solomon (9.5°S and 160°E), and Palau (7°N and 134.5°E), with the latitudes and longitudes stated giving the approximate locations of these islands or island groups. Since climate models do not have the greatest resolution over islands due to their small landmass, a squared domain of plus and minus 8° from the station's latitude and longitude point is used to get a more representative estimate of the changes in conditions in the vicinity of the islands. The domains of Central Polynesia, Micronesia, and Melanesia, which are the oceanic regions of interest, are big enough to give a good enough estimate of mean precipitation change. We also assess climate change in broader oceanic regions of the tropical Pacific in our analysis. These oceanic regional domains are highlighted in Figure 2.1.

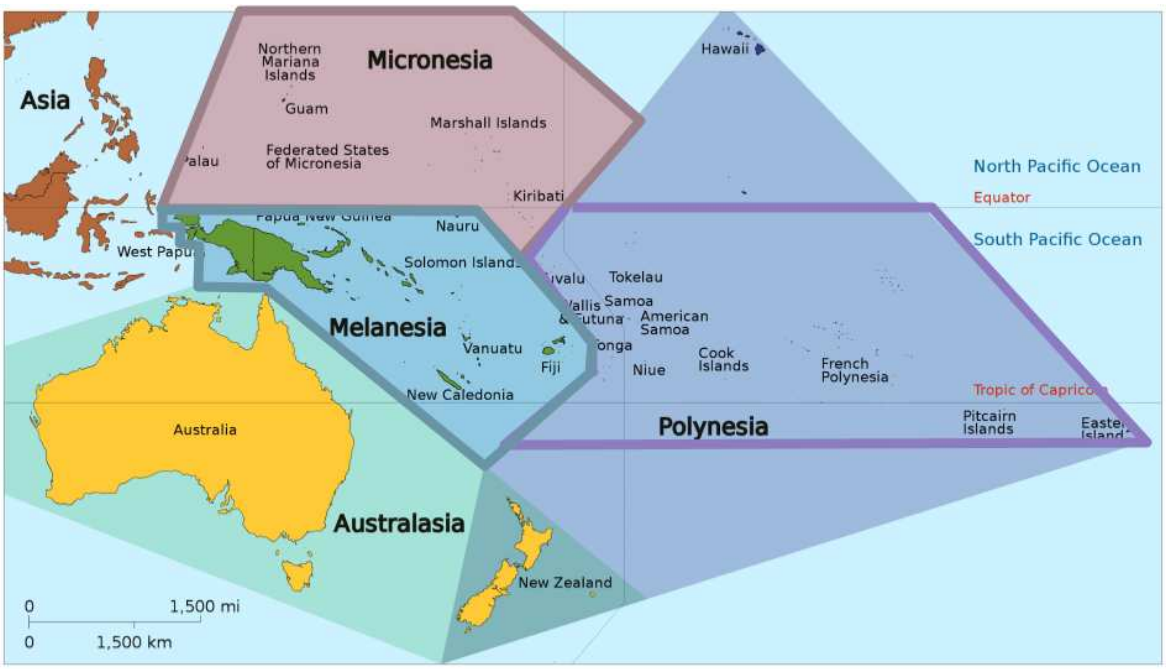

FIG. 2.1. Map of Oceanic Regions of interest are Central Polynesia, Micronesia, and Melanesia based on the United Nations geoscheme M49 coding classification devised by the United Nations Statistics Division

2.3 RESULTS AND DISCUSSION

2.3.1 PREFERENTIAL CONCENTRATION OF SST WARMING AND PRECIPITATION FORMATION

The period 1985-2005 is used as the reference historical period to assess climate changes in the projections, as shown in Figure 2.2. SST and precipitation pattern changes in future 20 year periods of 2021-2040, 2041-2060, 2061-2080, and 2081-2100 are analyzed in some of the analysis. Even though the base state that the investigation uses provides a reasonable baseline for assessing future climate changes, it does contain some biases as shown by Figure 2.2. For example, evidence for a double ITCZ bias exists, with precipitation bands too zonally-oriented across the Pacific. Many climate models with this bias tend to overestimate precipitation changes, thus skewing projections (Hwang and Frierson 2013). This investigation acknowledges that biases such as the double ITCZ add some questions about the validity of the projections, although we do not attempt to account for the effects of this bias in our analysis.

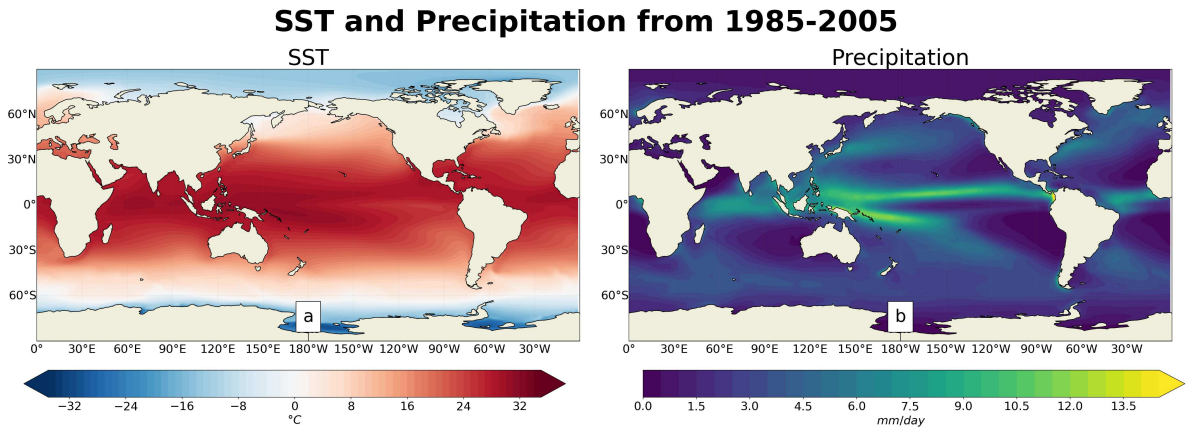

FIG. 2.2. Mean Sea Surface Temperature (SSTs) and Precipitation during the historical baseline period of 1985 to 2005

The mean SST (left) and precipitation (right) pattern change for examples of ensemble members that show preferential warming and precipitation changes weighted toward either the eastern, central, or western Pacific are shown in Figure 2.3, Figure 2.4, and Figure 2.5. It is worth noting that these figures use one ensemble member out of all 80 members to show the strongest preferential warming toward either Pacific region. The most stark differences by visual inspection out of all ensemble members are displayed. In earlier decades, for instance 2021-2040, while different ensemble members show the strongest preferential SST warming and precipitation changes weighted more toward the west, central, or east Pacific, east Pacific warming still tends to dominate in most members.

In 2021-2040, ensemble member #11 mean SST and precipitation pattern changes are most weighted toward the eastern Pacific, ensemble member #27 mean SST and precipitation pattern changes are most weighted toward the central Pacific, and ensemble member #67 mean SST and precipitation pattern changes are most weighted toward the western Pacific, as seen in Figure 2.3. The precipitation pattern changes follow to the first order the SST pattern changes. Thus, the preferential Pacific region uses the same singular ensemble member for both SST pattern change and precipitation pattern change for each 20-yr decadal period. In general, the qualitative nature of the warming pattern during 2021-2040 is affected more by decadal variability than later periods of the 21st Century, where a more El Niño-like warming pattern tends to dominate (see below).

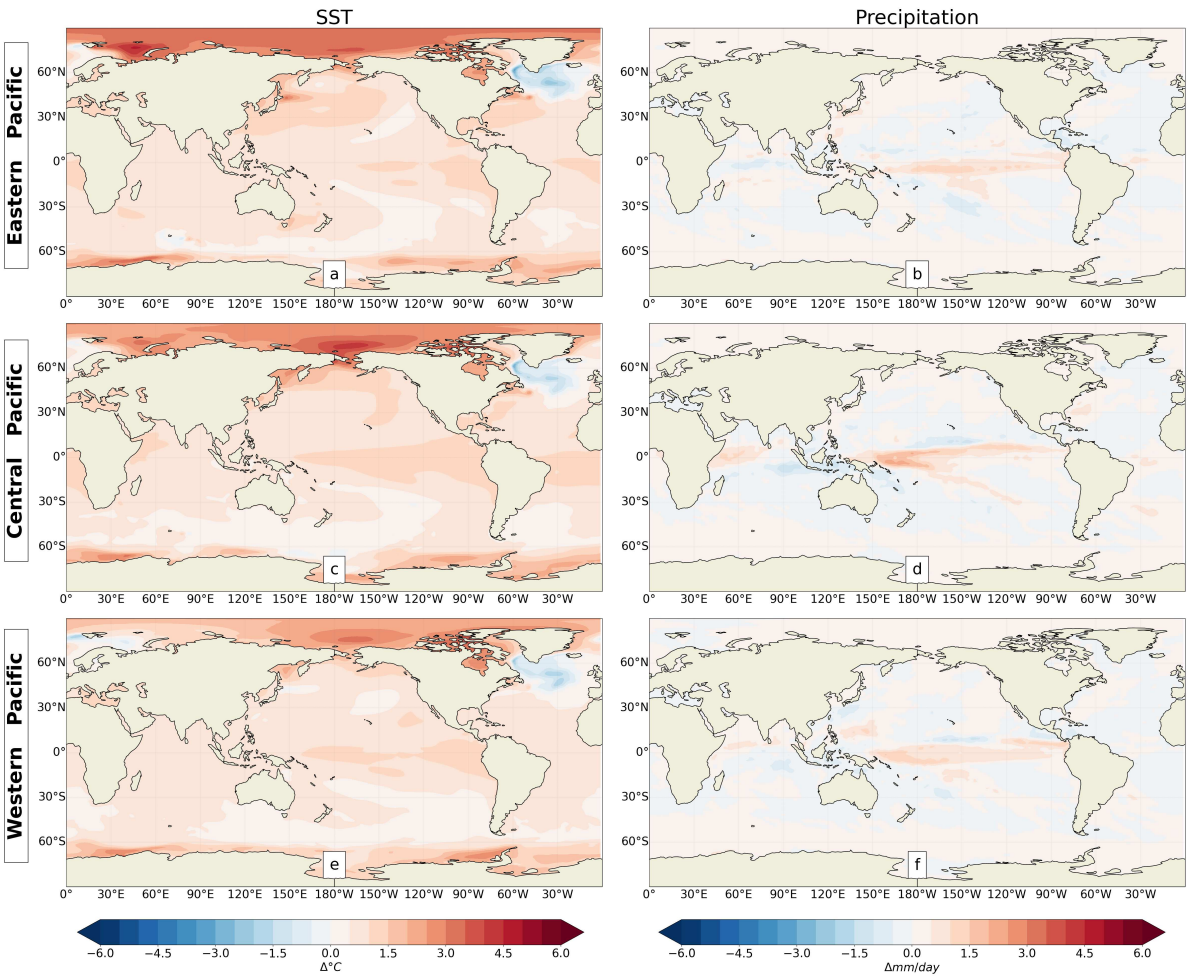

FIG. 2.3. Change of 2021-2040 Sea Surface Temperatures (SSTs) and Precipitation Relative to 1985 to 2005 for one ensemble member out of all 80 members that exhibit more east Pacific (top), central Pacific (middle), and west Pacific (bottom) warming

Later in the 21st century, these preferential warming and precipitation patterns become less distinctly different as the earlier 20-yr period. In the 2041-2060 period, ensemble member #10 mean SST and precipitation pattern changes are most weighted toward the east Pacific, ensemble member #46 mean SST and precipitation pattern changes are most weighted toward the central Pacific, and ensemble member #40 mean SST and precipitation pattern changes are most weighted toward the western Pacific, as seen in Figure 2.4. The classification of preferential warming and precipitation changes becomes harder to identity since all members show preferential warming toward the central and eastern Pacific Region. This tendency becomes even more apparent for the 2061-2080 period (Figure 2.5) and the 2081-2100 period (not shown). All ensemble members eventually show an El Niño-like warming

pattern at the midpoint of the 21st century and after, although there may still be subtle weighting toward one side of the basin.

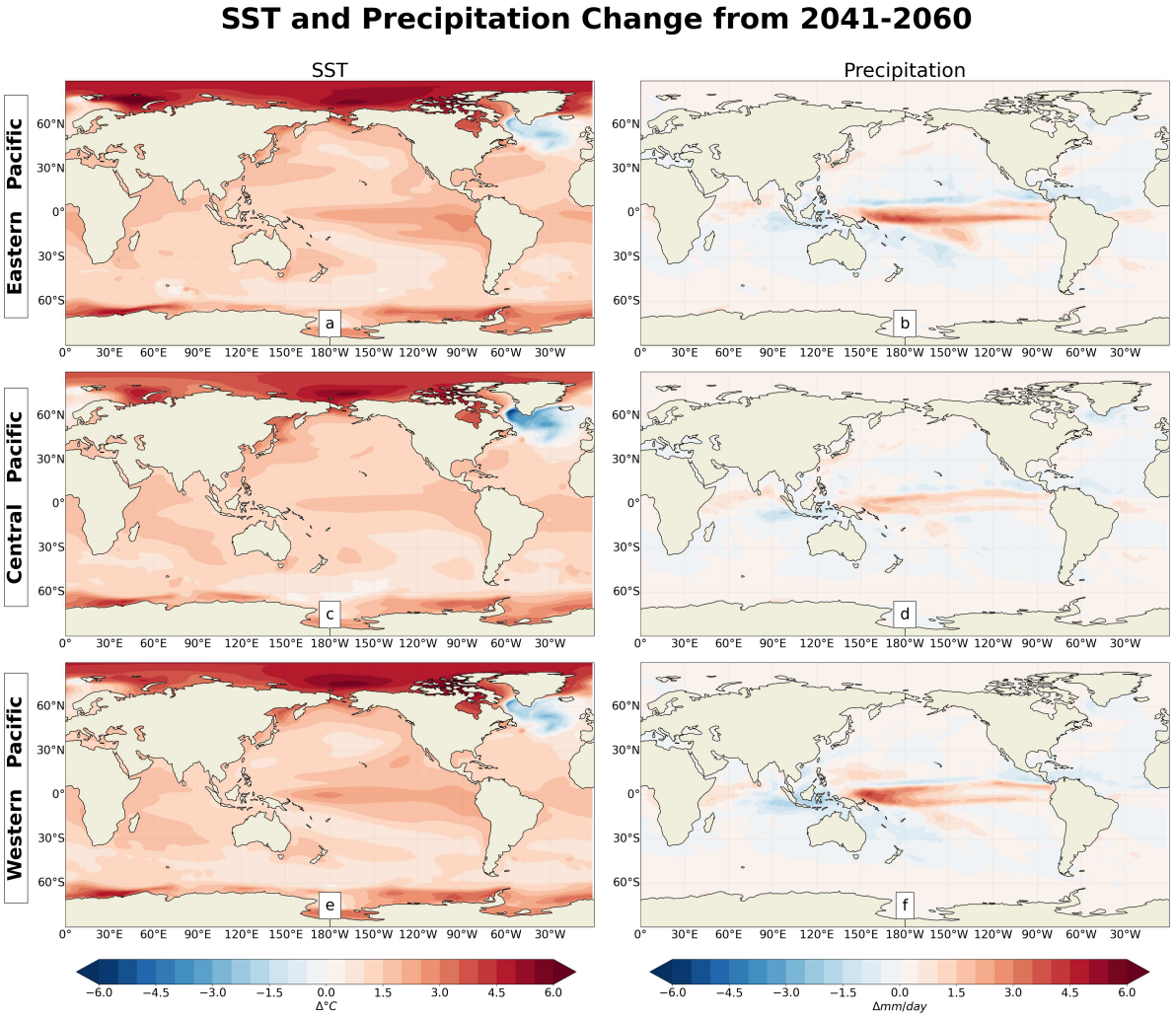

FIG. 2.4. Change of 2041-2060 Sea Surface Temperatures (SSTs) and Precipitation Relative to 1985 to 2005 for one ensemble member out of all 80 members that exhibit more preferential warming pattern to the east Pacific (top), central Pacific (middle), and west Pacific (bottom)

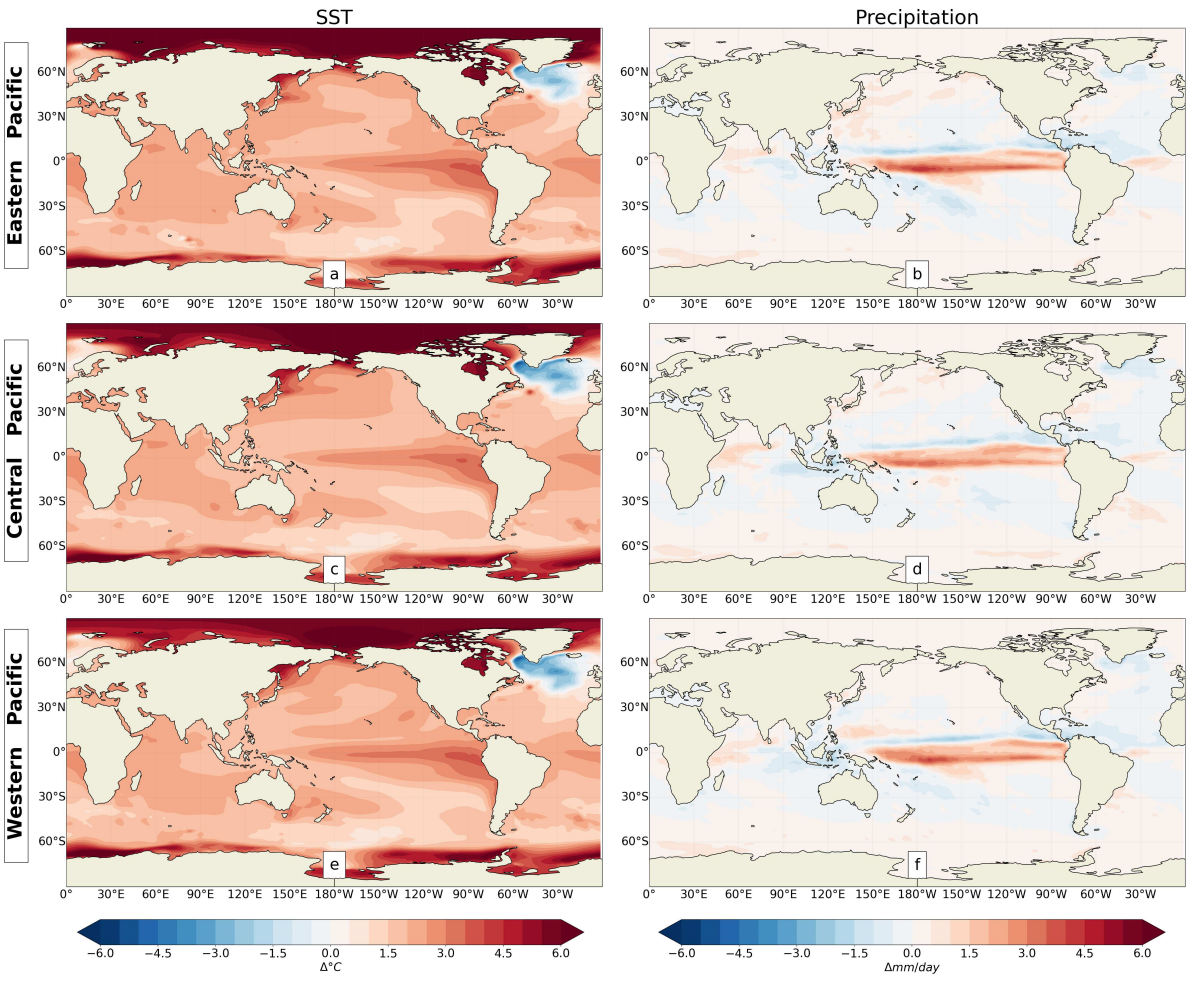

FIG. 2.5. Change of 2061-2080 Sea Surface Temperatures (SSTs) and Precipitation Relative to 1985 to 2005 for one ensemble member out of all 80 members that exhibit more preferential warming pattern to the east Pacific (top), central Pacific (middle), and west Pacific (bottom)

Future MJO changes are strongly sensitive to the pattern of warming, and this motivates examination of the MJO change in the models for different warming patterns (Takahashi et al. 2011), which will be discussed below. However, there are also important implications of these warming patterns on mean precipitation in tropical islands and ocean regions. Increasing El Niño-like warming favors enhanced rainfall in the central to eastern Pacific, and less in the western Pacific. Overall, these changes can impact global food security and livelihood for these vulnerable nations. However, the tendency of El Nino-like warming may not be quite as prominent earlier in the century (e.g. Figure 2.5). Thus, further objective analysis of these pattern changes using quantitative measures of SST pattern changes as they affect Pacific island stations is warranted.

2.3.2 Objective Measures of SST Pattern Changes in the Equatorial Pacific

While future projections resemble El Niño-like warming by the end of the 21st century in all ensemble members, nuances exist in the nature of the warming patterns, especially earlier in the century when warming can be more weighted toward the west Pacific. Thus, SST pattern changes are quantified using an index for the relative warming of east and west Pacific. Changes in mean precipitation at island stations is also examined to evaluate how mean precipitation change relates to uncertainty in SST patterns. The warming in the Niño3.4 region and the relative warming of the east Pacific relative to the west provide two measure of Pacific SST change in a warming climate, and hence these are also compared.

A positive value for tropical East minus West Pacific SST change implies the eastern Pacific is warming more than the western Pacific. Examination of Niño3.4 SST changes is useful as a reference of the absolute SST increase across ensemble members in the future climate. These two measures are computed using a 10-year running mean for each ensemble member, and compared to the historical period. Shading that spans the highest and lowest values across all 80 ensemble members is displayed in addition to the ensemble running mean to see the variability across ensemble members.

Tropical East-West Pacific SST gradient and Niño3.4 SST changes both show a positive overall trend with a rate increase of 0.08 and 0.18°C per 5 year period, respectively, as seen in Figure 2.6. While the relative SST change of the east Pacific versus the west gradient and Niño3.4 SST change generally go up relative to 1985-2005, the tropical East-West Pacific SST gradient change has a weaker consistent upward trend and wider uncertainty range. Notably, preferential west Pacific warming can occur in some of the members before 2055. Further, there is a larger ensemble member spread in the earlier period in both indices. This behavior indicates the importance of decadal variability for regulating the pattern of SST change. However, both tropical East-West Pacific SST gradient changes and Niño3.4 SST changes support more El Niño-like warming for all ensemble members toward the end of the 21st century. It is worth noting that model bias can be present, especially with the double ITCZ bias within models. The usage of detrending the data could help reduce this problem.

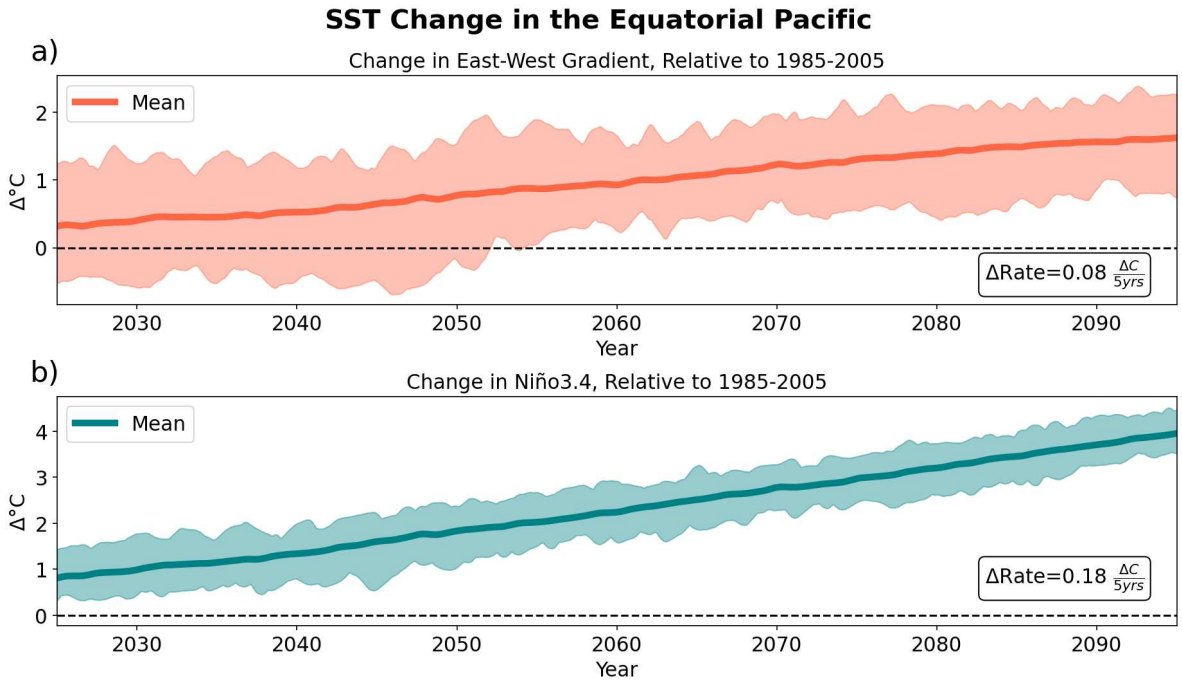

FIG. 2.6. Pattern Change of Sea Surface Temperatures (SSTs) in Niño3.4 and East-West Relative to 1985 to 2005 in the Pacific

2.3.3 PRECIPITATION PATTERN CHANGES OF PACIFIC ISLANDS AND OCEANIC REGIONS

Pacific oceanic regions and their associated islands heavily rely on precipitation as a freshwater source. Future precipitation change can affect the livelihoods of these isolated locations, and projection information can help people prepare. The analysis of station precipitation informs how these islands' water resources may eventually change, especially with ensemble members indicating an SST warming pattern change that is El Niño-like. The station precipitation changes relative to historical period are displayed using a 10-year running mean for each ensemble member, with the cone of uncertainty resulting from ensemble member variability.

Islands such as Guam, Samoa, Kirbati, Galapagos Islands, Solomon, and Palau are equatorial Pacific stations of interest due to their diversity of locations across the tropics. Island precipitation changes show different behavior among stations until the end of the 21st century, as seen in Figure 2.7. Guam has a weak negative trend with a rate decrease of 0.15 $\frac{mm}{day}$ every 80 years in Figure 2.7 a. Samoa has a moderate positive trend with a rate increase of 0.66 $\frac{mm}{day}$ every 80 years in Figure 2.7 b. Kirbati has a strong positive trend with a rate increase of 1.64 $\frac{mm}{day}$ every 80 years in Figure 2.7 c. Galapagos has a strong positive trend with a rate increase of 1.74 $\frac{mm}{day}$ every 80 years in Figure 2.7 d. Solomon has a moderate positive trend with a rate increase of 0.57 $\frac{mm}{day}$ every 80 years in Figure 2.7 e. Palau has a weak

negative trend with a rate decrease of 0.3 $\frac{mm}{day}$ every 80 years in Figure 2.7 e. The positive trends are associated with islands located more in the central and eastern Pacific, with the strongest trends located closest to the equator. However, the negative trends are seen more in the western Pacific, which is consistent with what is expected from an El Niño-like SST pattern change and associated change in precipitation patterns, as shown in Section 2.3.1.

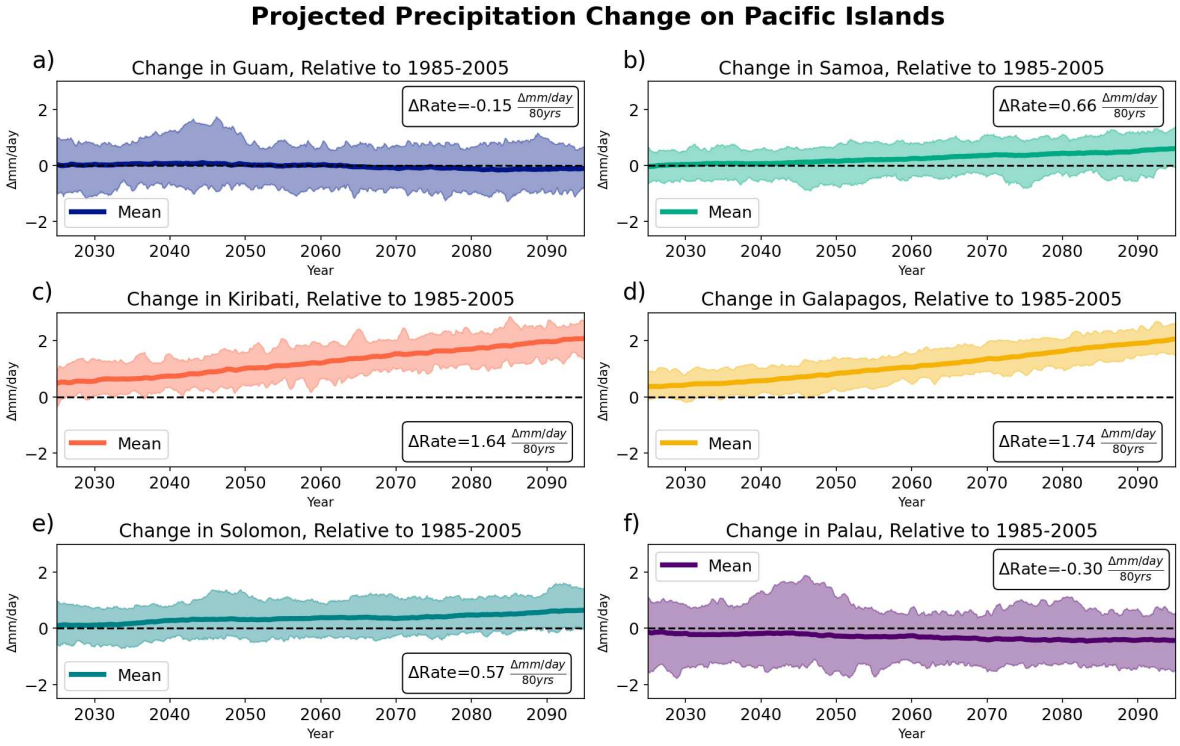

FIG. 2.7. 10-yr running mean of rainfall rate relative to 1985 to 2005 for Pacific Islands a) Guam, b) Samoa, c) Kirbati, d) Galapagos Islands, e) Solomon, and f) Palau

The magnitude of the ensemble spread for each island precipitation also varies. The western and central Pacific islands tend to have a higher range of variability across ensemble members than the eastern Pacific. In addition, the islands located in higher latitudes have smaller variability. The Galapagos has the smallest ensemble variability out of all the Pacific Islands, suggesting more certainty for future projections in this region.

Precipitation changes for broader oceanic regions of interest including Central Polynesia, Micronesia, and Melanesia are shown in Figure 2.1. Mean precipitation changes from various oceanic region also show different trends over the 21st century. All oceanic regions of interest shown here have positive trends, but vary in strength seen in Figure 2.8. Central Polynesia has a moderate rate increase of 0.69 $\frac{mm}{day}$ every 80 years in Figure 2.8 a. Micronesia has a weak rate increase of 0.2 $\frac{mm}{day}$ every 80 years in

Figure 2.8 b. Melanesia has a moderate rate increase of 0.54 $\frac{mm}{day}$ every 80 years in Figure 2.8 c. Thus, Central Polynesia, which is located in the central to eastern Pacific has the strongest positive trend of mean precipitation change out of all the oceanic regions. In contrast, Micronesia, which is located in the northwest Pacific has the weakest positive trend. It is notable that the lower bound on the ensemble spread rises above the zero change line for both Melanesia and Central Polynesia toward the end of the 21st Century. While the overall Micronesia and Melanesia trend is a weak to moderate positive trend, the islands located in these region seen in Figure 2.7 shows a negative trend. Hence, especially in the western Pacific, individual islands can have different of precipitation changes than the overall domain.

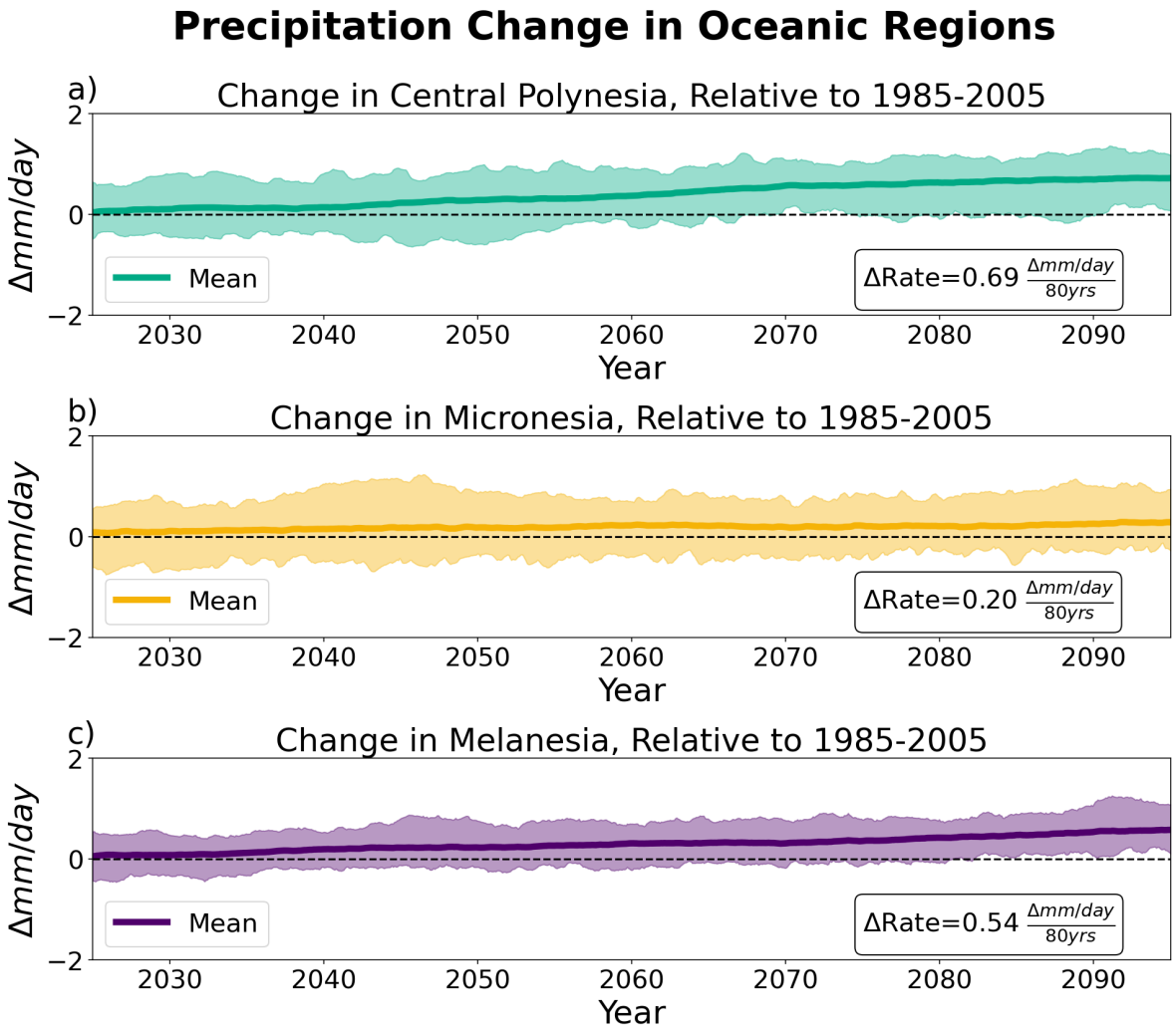

FIG. 2.8. 10-yr running mean of rainfall rate change relative to 1985 to 2005 for Oceanic Regions a) Central Polynesia, b) Micronesia, and c) Melanesia

2.4 CONCLUSION

Decadal variability in the climate system affects the pattern of SST change in projections with the CESM2 LENS from one decade to the next and across ensemble members. The details of the SST pattern change strongly influence the patterns of precipitation change during any given period within an ensemble member, for example, as shown in Figure 2.4. Earlier decades of the 21st Century show SST warming that can be more weighted toward the west, central, or east Pacific, although all ensemble members eventually show an El Niño-like warming pattern in later decades. While Niño3.4 SST and the tropical East-West Pacific SST gradient change generally go up relative to 1985-2005, the Niño3.4 SST pattern change has a much stronger consistent upward trend and tropical East-West Pacific SST gradient pattern change has a wider range of variability, with some ensemble members showing preferential west Pacific warming earlier in the 21st Century. An El Niño-like warming pattern eventually emerges across all ensemble members in the later half of the 21st Century.

Islands distributed across the tropical Pacific have various magnitudes of mean precipitation change for each individual station. Positive precipitation trends generally occur for islands located in the central and eastern Pacific with the strongest trends located closest to the equator, but negative trend for islands in the western Pacific. Island precipitation change is generally consistent with the long-term trend in projected central and eastern Pacific warming. However, islands in the west Pacific have uncertain signs of precipitation change across individual ensemble members, which provides uncertainty in future climate projections. This makes it challenging to predict future changes in water resource availability for tropical islands. While high resolution models would be able to better isolate the details of island precipitation change, because a coarser Earth system model was used here, this investigation gives an estimate of the more general behavior of precipitation change in the vicinity of individual islands. Broader oceanic regions were also examined. Central Polynesia has the strongest positive mean precipitation trend, while in contrast, Micronesia has the weakest positive trend. While Micronesia and Melanesia trends are positive, the individual Pacific islands located in these regions that were examined have a negative precipitation change trend. However, western Pacific precipitation changes have large scatter across ensemble members and trends are overall likely not statistically significant. This highlights high uncertainty in precipitation projections for tropical Pacific islands, particularly for the west Pacific. Changes for the east Pacific islands like the Galapagos are more robust, with increasing El Niño-like warming and precipitation trends toward the end of the 21st Century.

These results lead into the next chapters about how these projected SST pattern changes influence MJO activity in a future climate. The next chapter (Section 3) aims to analyze how the pattern of projected SST change is related to changes in MJO activity. Section 4 investigates how changes to the mean vertical moisture profile and horizontal SST and moisture profile help to explain these changes.

CHAPTER 3

MJO ACTIVITY IN A FUTURE WARMER CLIMATE

3.1 CHAPTER 3 PRELUDE

The investigation discusses how projected SST pattern changes influence MJO Activity as defined by MJO precipitation and wind amplitude changes. The distribution of MJO precipitation and wind amplitudes changes relative to the historical period are analyzed. The impact of projected SST pattern changes on MJO activity is then examined, including the relationship to the degree of SST change in the Niño3.4 region. The impact of projected Niño3.4 SST changes on MJO activity in specific oceanic regions of interest is also examined.

Ultimately, this investigation examines how SST pattern changes influence MJO activity in the tropics, as well as the implications of decadal variability. The proposed investigation questions are (1) how does the ensemble mean spatial distribution of MJO precipitation and wind amplitude change in a warmer climate? (Section 3.3.1), (2) to what extent does the pattern of projected SST change influence MJO precipitation and wind amplitude? (Section 3.3.2), and (3) how does MJO amplitude change affect specific oceanic island regions in a warmer climate? (Section 3.3.3).

3.2 DATA AND METHODOLOGY

Eighty CESM2 ensemble members with the radiative forcing scenario SSP370 are used for the investigation (Riahi et al. 2017; Rodgers et al. 2021), as in the prior section, and so more details on the model runs are contained there.

MJO activity can be diagnosed using various variables including precipitation, net outgoing longwave radiation (OLR), and upper level and lower level zonal winds (Madden and Julian 1994; Wheeler and Kiladis 1999). MJO activity and its changes in this investigation are defined using precipitation and 850 mb zonal wind. MJO variability is isolated by detrending the data in individual variables, removing the seasonal cycle, and applying a frequency-wavenumber bandpass filter to the dataset (Madden and Julian 1994; Wheeler and Kiladis 1999). The data is detrended by least squared regression fit. The frequency-wavenumber domain shows a strong MJO signal for 30-90 days frequency, 1-5 zonal wavenumber (k) (Wheeler and Kiladis 1999). MJO signals in precipitation and 850 mb zonal wind are isolated by a bandpass filter for this region of the frequency-wavenumber domain (Bingham et al. 1967). The standard deviation of this filtered precipitation and zonal wind dataset defines MJO amplitude, or activity, for the rest of the investigation.

Since the MJO propagates eastward over the Tropics, the investigation evaluates MJO amplitude change domain over the entire tropics (15°S - 15°N). The investigation first evaluates ensemble mean MJO amplitude change through the filtered precipitation and zonal wind at 850 mb relative to 1985-2005 for future 20 year periods of the 21st century. Standardized MJO amplitude changes are also examined, defined by the percentage change (3.1) in continuous 20-year decadal periods: 2021-2040, 2041-2060, 2061-2080, and 2081-2100 relative to the historical period, consistent with Bui and Maloney (2018).

$$PercentageChange = \frac{\bar{X}_{future} - \bar{X}_{1985-2005}}{\bar{X}_{1985-2005}} * 100, \tag{3.1}$$

The investigation then evaluates scatterplots of each ensemble member's MJO amplitude change versus degree of east Pacific warming defined by Niño3.4 for each 20-year period. Pearson's correlation is used to measure the strength and direction of the linear covariance between the two variables, in this case, SST Niño3.4 change and MJO amplitude change over the tropics for individual ensemble members.

Maps of SST change for the 33% of ensemble members with biggest MJO amplitude increases (MJO plus) minus the bottom 33% (MJO minus) is useful to assess how the SST change pattern differs between these, for direct comparison with Takahashi et al. (2011). A two-tailed t-test is also applied to assess the significance difference between the MJO plus and MJO minus maps for each 20-year decadal period.

This investigation not only focuses on SST pattern changes, but also MJO activity responses on vulnerable oceanic island regions and their communities Mycoo et al. (2022). The oceanic regions of interest are Central Polynesia, Micronesia, and Melanesia, as seen in Figure 2.1. The investigation assesses the relationship between MJO activity changes in the oceanic regions of interest and projected Niño3.4 SST warming for each 20-year decadal period Trenberth (1997).

3.3 Results and Discussion

3.3.1 MJO Activity Change in a Future Climate

The ensemble mean MJO precipitation and 850 mb zonal wind amplitude for 1985-2005 shows higher values in the Indo-Pacific warm pool, as seen in Figure 3.1. The percentage change of the ensemble mean precipitation and wind amplitudes is shown in the bottom panels for different periods of the 21st Century. MJO precipitation and zonal wind amplitude percentage changes are positive, and

get stronger in the central to eastern Pacific for each future 20-yr decadal period in a warmer climate (Figure 3.1). The strongest percentage change signal for MJO precipitation and zonal wind 850 mb is seen in 2081-2100. Thus, in the CESM2 ensemble mean, MJO amplitude increases in intensity in a future climate. Moreover, the MJO precipitation percentage change is stronger than zonal wind change, consistent with that expected under WTG theory Bui and Maloney (2018). The pattern of MJO precipitation and zonal wind trends is consistent with the response to an El Niño-like warming pattern (e.g. Figure 3.2).

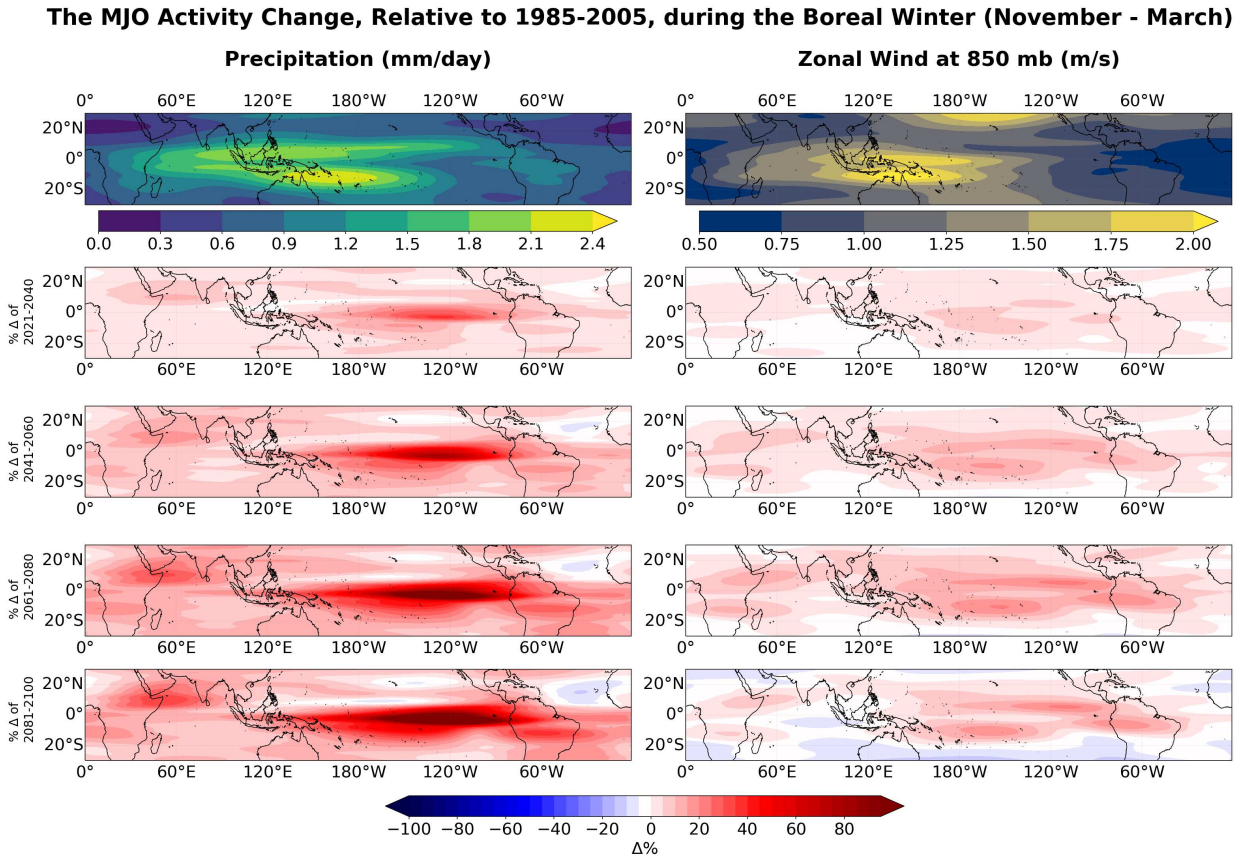

FIG. 3.1. Top row: Ensemble mean MJO precipitation and 850 mb zonal wind standard deviation for the 1985-2005 period. Bottom rows, the percentage change in MJO Activity relative to 1985 to 2005 based on 20-yr decadal periods.

One question is whether the MJO amplitude change in individual ensemble members tracks with the degree of warming in the ENSO region. The correlation between the Niño3.4 region SST index change and MJO amplitude across ensemble members is examined. The correlation between the Niño3.4 SST change and the MJO precipitation amplitude change (averaged across the entire Tropics) indicates a significant positive relationship for 2041-2060 and 2081-2100, as seen in Figure 3.2. However, a large

spread exists. Internal MJO variability is likely the cause of the large spread, which reduces the strength of the correlation. The correlations between wind amplitude change and SST change are predictably weaker, consistent with WTG theory and increases in static stability of the tropics in response to warming (Maloney et al. 2019). For example, in 2041-2060 there is a moderate positive correlation of 0.45 between Niño3.4 SST change and MJO precipitation amplitude change, but a weaker positive correlation of 0.3 between Niño3.4 SST and MJO zonal amplitude change. In 2081-2100, there is a weak positive correlation of 0.31 between Niño3.4 SST and MJO precipitation amplitude change, but an extremely small correlation of 0.07 between Niño3.4 SST and MJO zonal wind change. Notable is that the highest correlations for SST versus MJO precipitation and zonal wind changes tend to occur earlier in the 21st Century in 2041-2060, when the pattern of SST change is still strongly regulated by decadal variability across ensemble members. Correlations between the change in the tropical Pacific SST gradient and MJO precipitation and wind amplitude produce similar results to those described here (not shown). The pattern of SST change associated with the ensemble members having biggest MJO amplitude increases is investigated next.

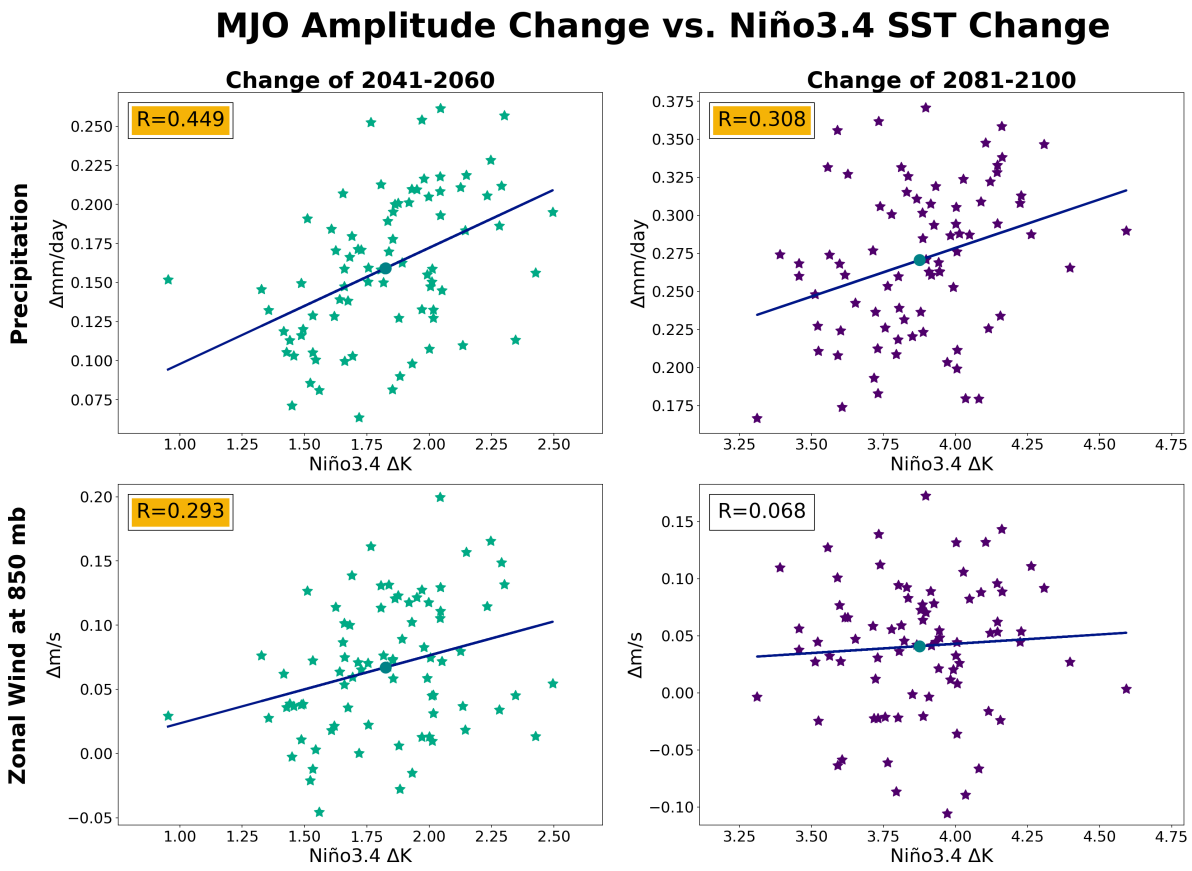

FIG. 3.2. MJO amplitude change versus Niño3.4 SST Change. Precipitation and 850 mb zonal wind amplitude change across the entire Tropics relative to 1985 to 2005 is shown for two 20-year periods

3.3.2 SST PATTERN CHANGES FOR THE STRONGEST MJO AMPLITUDE CHANGES

"MJO plus" ensemble members refer to those with the top 33% changes of MJO precipitation and 850 hPa zonal wind amplitude averaged across the tropics (15°N - 15°S), while "MJO minus" refers to the ensemble members with bottom 33% of change. Difference in the SST pattern change between MJO plus and minus members indicates that greater MJO precipitation amplitude increase is associated with a more El Niño-like warming pattern, as seen in Figure 3.3, as well as more warming in the MC region where the MJO propagates east (Kim et al. 2017). The pattern is generally consistent with that found by Takahashi et al. (2011) in CMIP3 models. A stronger meridional SST gradient is implied for in the western to central Pacific for ensemble members with stronger MJO precipitation amplitude increase, which will be investigated further below, as there may be implications for the moisture gradient field that regulates eastward MJO propagation. A two-tailed t-test of difference of means between MJO plus and MJO minus members at the 95% confidence level indicates that stronger warming in the

central and eastern equatorial Pacific for MJO plus members is generally statistically significant. For zonal wind amplitude change, the SST pattern change for those with biggest amplitude increases is less robust than for precipitation, consistent with the generally less interesting and robust response of MJO wind amplitude to climate warming.

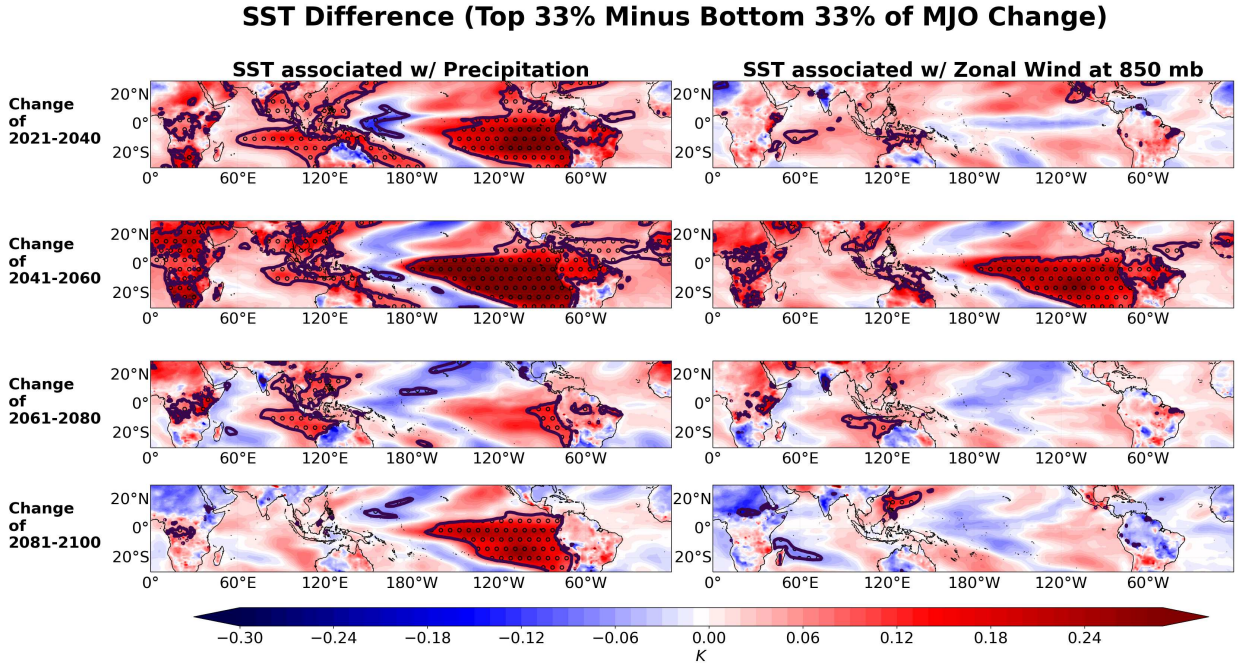

FIG. 3.3. Difference in SST change for the ensemble members with top 33% of MJO amplitude change (MJO Plus) minus the bottom 33% of MJO amplitude change (MJO Minus). Precipitation and zonal wind amplitude changes are analyzed for different 20 yr periods

3.3.3 MJO ACTIVITY VERSUS SST IN OCEANIC REGIONS

The evaluation of MJO amplitude change for specific oceanic regions such as Central Polynesia, Micronesia, and Melanesia seen in Figure 2.1 helps to elucidate the change in MJO impacts for these vulnerable communities in a warming climate. The correlation between the Niño3.4 SST change and MJO amplitude changes in oceanic regions are generally positive and above 0.3, indicating that ensemble members with more El Niño-like warming will have bigger MJO impacts in these regions. In 2041-2060, the relationship between SST change and MJO amplitude is statistically significant for Central Polynesia, which is more located in central to eastern Pacific, and Micronesia, which is weighted toward the Northern Hemisphere of the western Pacific seen in Figure 3.4. In 2081-2100, the relationship between Niño3.4 SST change and MJO amplitude change is statistically significant for Central

Polynesia and Melanesia, which are weighted toward the Southern Hemisphere of the western Pacific seen in Figure 3.5. As stated before, the large spread is likely influenced by internal MJO variability.

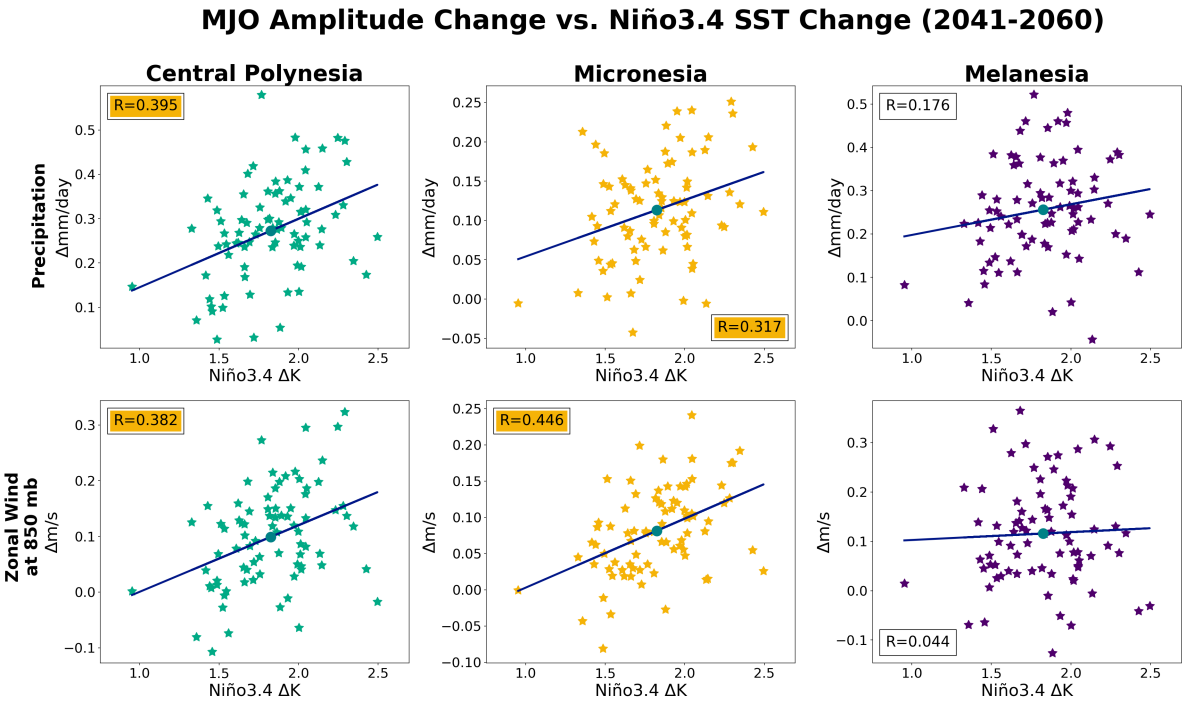

FIG. 3.4. Relationship between Niño3.4 Sea Surface Temperatures Change and MJO amplitude change for three oceanic regions: Central Polynesia, Micronesia, and Melanesia for 2041-2060. Precipitation and zonal wind amplitude changes are analyzed. Correlations that are shaded are statistically significant.

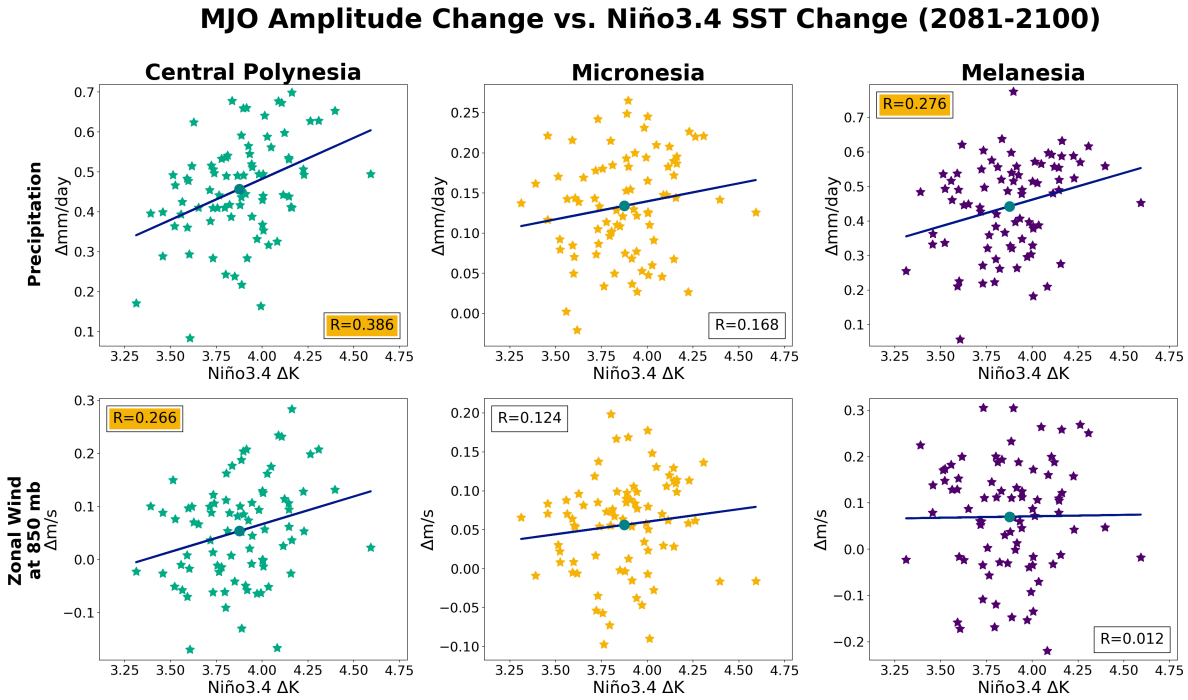

FIG. 3.5. Same as Figure 3.4, but for 2081-2100.

3.4 CONCLUSION

The ensemble mean shows that MJO precipitation and wind amplitude increases in a warming climate in CESM2. Future projections show that the strongest MJO activity change occurs in the central to eastern Pacific. CESM2 Ensemble members with the greatest tropics-wide MJO amplitude increase have a more El Niño-like warming pattern. This warming pattern also suggests a stronger meridional SST gradient in the western to central Pacific, in addition to the greater SST warming in the east Pacific on the equator.

Viewed through the lens of moisture mode theory, these characteristics of the SST pattern change for members with higher MJO amplitude increase might be expected to have impacts on the basic state moisture field and thus affect MJO maintenance and propagation. Research questions focusing on moisture changes are explored in next chapter, particularly related to how changes to mean vertical and horizontal moisture profiles affect MJO activity in the context of such SST pattern change.

CHAPTER 4

VERTICAL MOISTURE EFFECT ON MJO ACTIVITY IN A FUTURE WARMER CLIMATE

4.1 CHAPTER 4 PRELUDE

The prior chapter showed that ensemble members with the biggest MJO amplitude change are associated with a warming pattern that is more El Niño-like. This warming pattern is likely to have impacts on the mean moisture field that affects MJO dynamics. The chapter will discuss projected vertical and horizontal moisture pattern changes and their influence on MJO amplitude in a warmer climate, as a way to explain why some ensemble members show greater MJO amplitude increases. The relationship between projected precipitable water changes and MJO amplitude change for the highest amplitude change members will be examined, especially the impact of meridional and vertical moisture profile change.

The proposed investigation questions are (1) how does the ensemble mean precipitable water pattern change in a warmer climate? (Section 4.3.1), (2) to what extent does the pattern of projected precipitable water change and its meridional gradient and vertical moisture profile change influence MJO precipitation and wind change in the Tropics? (4.3.2 and Section 4.3.3), and (3) what do meridional moisture gradients and vertical moisture profile changes look like for the ensemble members with biggest MJO amplitude change? (Section 4.3.3).

4.2 DATA AND METHODOLOGY

The same 80 CESM2 ensemble members with SSP370 forcing are used in this investigation, as in Chapter 3. The same method to isolate MJO amplitude and their changes is also used. The projected precipitable water (TMQ) pattern change is analyzed in 20-year periods: 2021-2040, 2041-2060, 2061-2080, and 2081-2100 (Wheeler and Hendon 2004; Gottschalck 2014; Bui and Maloney 2018). MJO plus and minus ensemble members denoting members with the largest and smallest MJO changes are again used, with the difference in TMQ change assessed for members with the largest MJO changes relative to the smallest (Takahashi et al. 2011). A more detailed analysis of TMQ meridional gradient changes and vertical humidity profile change for these members is also conducted. The TMQ meridional gradient change for the western and central Pacific is isolated (140°E to 150°W and 10°S to 10°N), as this region sees the most prominent TMQ change for the ensemble members with the strongest increase in MJO activity, and the meridional gradient in this region is likely important for influencing MJO propagation across the Pacific in a warmer climate. Scatterplots of meridional moisture gradient change

and lower tropospheric humidity change versus MJO amplitude change across ensemble members are also assessed. Significance testing on the correlation coefficients is also conducted.

4.3 Results and Discussion

4.3.1 Precipitable Water in a Future Climate

Integrated vertical moisture, precipitable water (TMQ), describes the amount of moisture contained in an atmospheric column, which is examined because moisture mode theory highlights the importance of tropospheric water vapor for regulating MJO dynamics. Figure 4.1 shows the ensemble mean TMQ pattern for the historical period, which generally follows the SST and precipitation patterns (e.g. Figure 3.2). The mean TMQ shows the strongest signal over the Indo-Pacific warm pool. Hints of a double ITCZ bias are seen in the TMQ pattern in the historical period, consistent with the precipitation pattern (Figure 3.2). The percentage change of TMQ is also shown in Figure 4.1. Overall, in a warmer climate, the CESM2 TMQ ensemble mean change has a moistening pattern with largest increase in the central to eastern Pacific, consistent with an El Niño-like warming pattern (Figure 4.1). The strongest TMQ amplitude change is in the 2081-2100 period, consistent with the SST change in Figure 3.2.

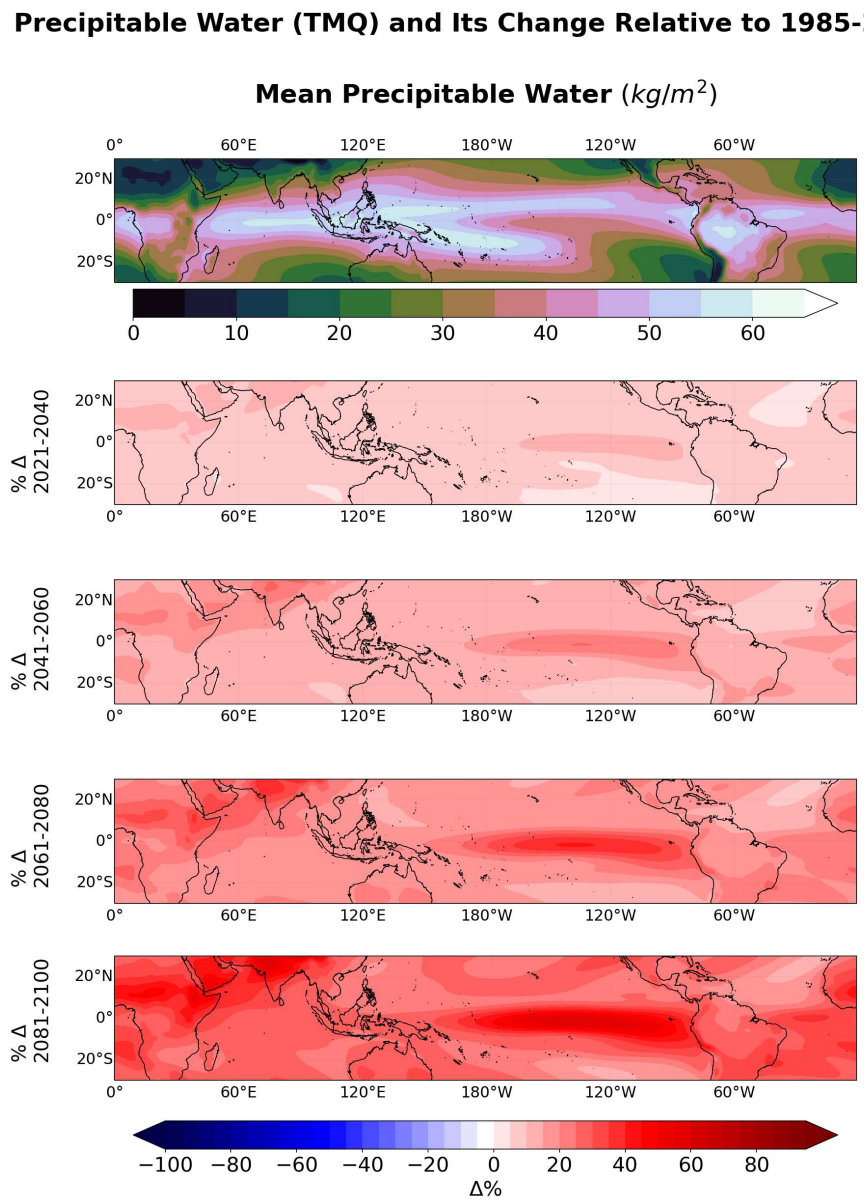

FIG. 4.1. Historical (1985-2005) precipitable water distribution (top panel) and its percentage change relative to the historical period (bottom panels)

4.3.2 MJO ACTIVITY PLUS AND MINUS OF PRECIPITABLE WATER

The precipitable water change for the members with biggest MJO amplitude increases are now compared to those with the smallest increases. Higher, statistically significant regions of TMQ in the central to eastern Pacific favor stronger MJO amplitude seen in Figure 4.2. The members with strongest MJO precipitation amplitude increase have a moisture pattern change that is more El Niño-like and mimics the SST pattern change, with greater moistening in the east Pacific and MC region, and suggestions of a stronger meridional moisture gradient in the western and central Pacific. The usage of

a two-tailed t-test between MJO plus and MJO minus members at the 95% confidence level indicates the central and eastern equatorial Pacific relative moistening and off-equatorial drying is statistically significant across all future periods. Moisture field changes associated with the greatest MJO wind amplitude changes are less robust, although tend to have an El Niño-like moistening pattern with only large regions of significance in the 2041-2060 period, similar to Figure 3.2. Similar to Figure 3.2, the largest regions of significance and the most robust TMQ change differences between MJO plus and minus members is in 2041-2060, for both MJO precipitation and zonal wind amplitude change. The investigation next dives into the TMQ meridional gradient field to reinforce its importance supporting MJO amplitude increases.

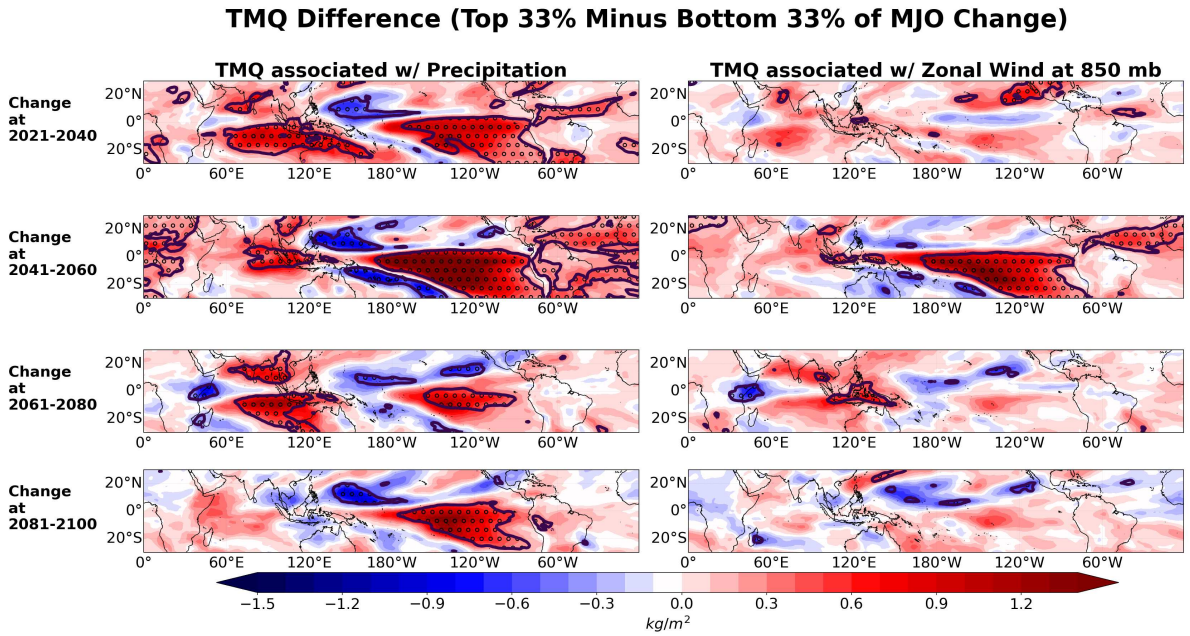

FIG. 4.2. Same as Figure 3.3, except for TMQ

As discussed in the introduction, a stronger meridional humidity gradient supports increased horizontal advection through the MJO meridional wind acting on the mean humidity gradient, which supports eastward MJO propagation (Maloney 2009). Differences in the meridional humidity gradient change between members with the strongest and smallest MJO amplitude changes are now examined. As shown in Figure 4.3, the TMQ meridional gradient difference between MJO plus and minus members for precipitation amplitude change indicates notable, significant differences across the equatorial Pacific, especially during the 2041-2060 period. The stronger TMQ meridional gradient for ensemble members with larger MJO amplitude change is consistent with stronger support for MJO propagation

across the Pacific through meridional moisture advection by the anomalous MJO flow (Adames and Kim 2016). The signal for MJO wind amplitude change is weaker, consistent with the discussion above.

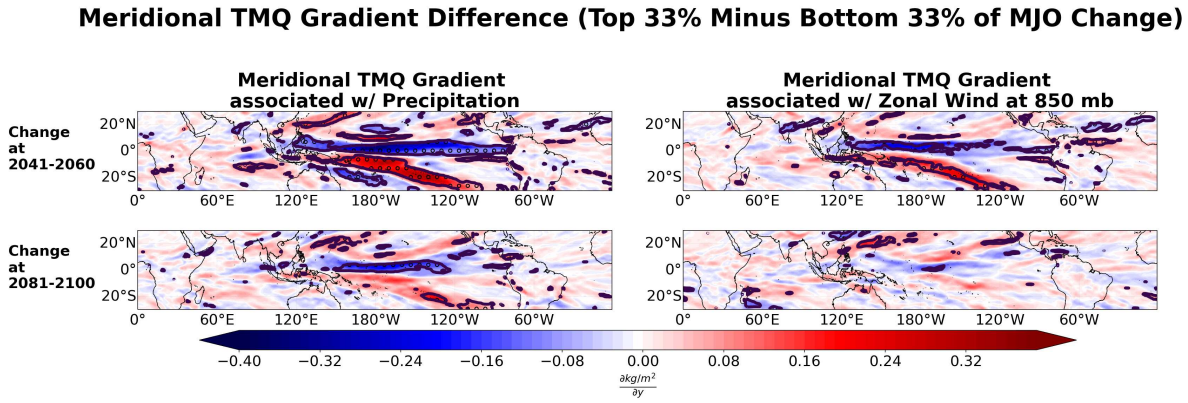

FIG. 4.3. Same as Figure 4.2, except for TMQ gradient

One question is whether a stronger meridional moisture gradient for individual members consistently produces an increased MJO amplitude. An analysis of correlations between Central Pacific TMQ meridional gradient change and tropical MJO precipitation amplitude change shows that there is a modest positive, statistically significant correlation (Figure 4.4). Note that the absolute value of the TMQ gradient was taken before averaging in the central Pacific box, such that the Northern and Southern Hemisphere gradients are treated equivalently. The relationship with 850 mb zonal wind amplitude change is not significant. It is worth noting again that substantial spread exists due to internal MJO variability. While there is a weak positive but significant relationship between central Pacific TMQ meridional gradient change and MJO precipitation amplitude change, other factors may also help to explain increases in MJO amplitude for some ensemble members. The following subsection examines whether changes to the vertical profile of moisture helps to explain preferential increases in MJO activity for some members.

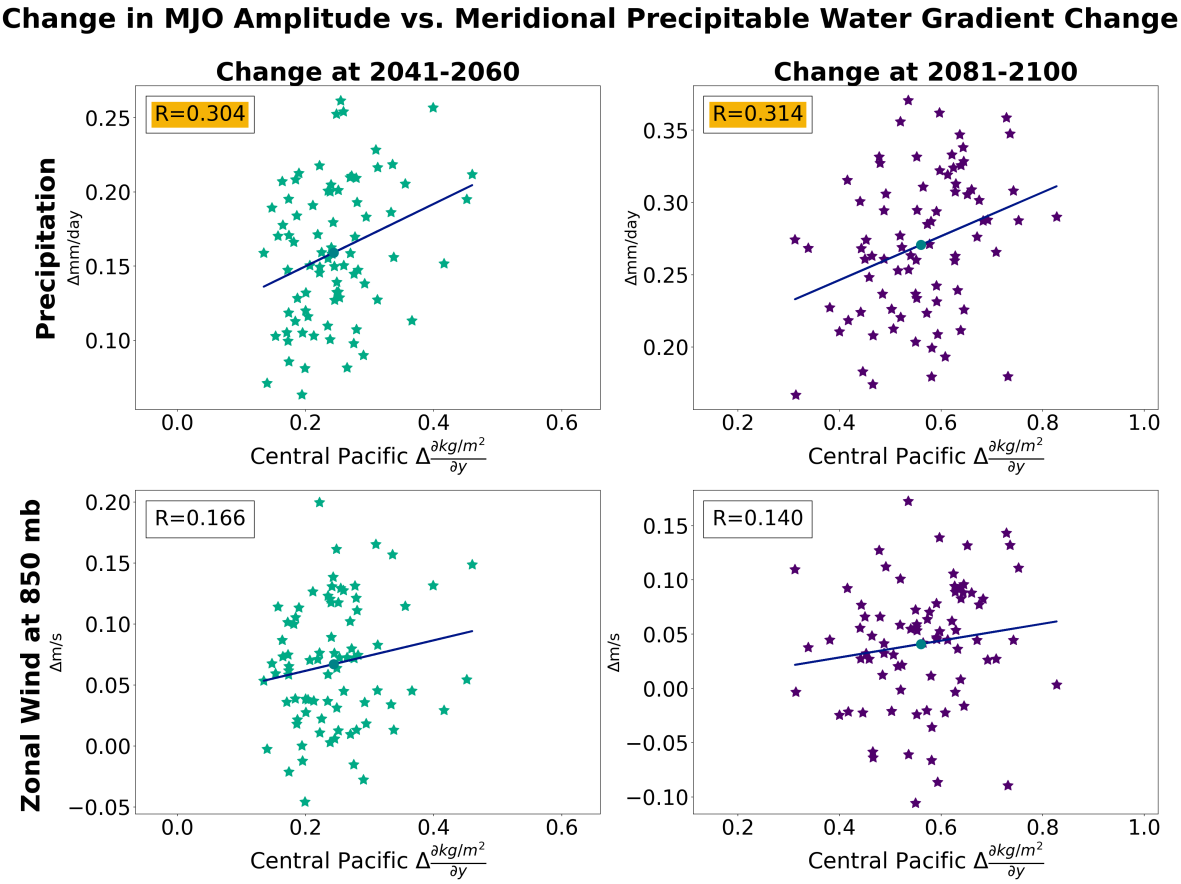

FIG. 4.4. Relationship between MJO amplitude change averaged over the entire tropics and Central Pacific TMQ meridional gradient change for precipitation and 850 mb zonal Wind relative to 1985 to 2005 for two 20-yr periods

4.3.3 VERTICAL MOISTURE PROFILE INFLUENCING MJO ACTIVITY

This investigation examines the difference in mean tropical Pacific specific humidity profiles isolated at the Equatorial Pacific (140°E to 81 °W and 10°S to 10°N) for the Pacific between MJO plus and minus members. Members with stronger MJO precipitation amplitude change have moister equatorial Pacific profiles, especially in the lower troposphere (Figure 4.5). This tendency is most notable for 2041-2060. The left panel of Figure 4.5 suggests stronger vertical moisture gradients for model simulations with increased MJO precipitation amplitude, consistent with that expected from prior studies (Arnold et al. 2015). The difference in moisture between MJO plus and minus wind amplitude change is not as pronounced as for precipitation amplitude change. A moistening signal only exists for 2041-2060 in wind amplitude, although this might only be due to internal variability. In general, the change in MJO precipitation amplitude between MJO plus and minus members is associated with a moister

equatorial troposphere and increased vertical humidity gradient, which would support MJO precipitation amplitude through more efficient moistening by vertical advection by MJO circulations (Maloney et al. 2019).

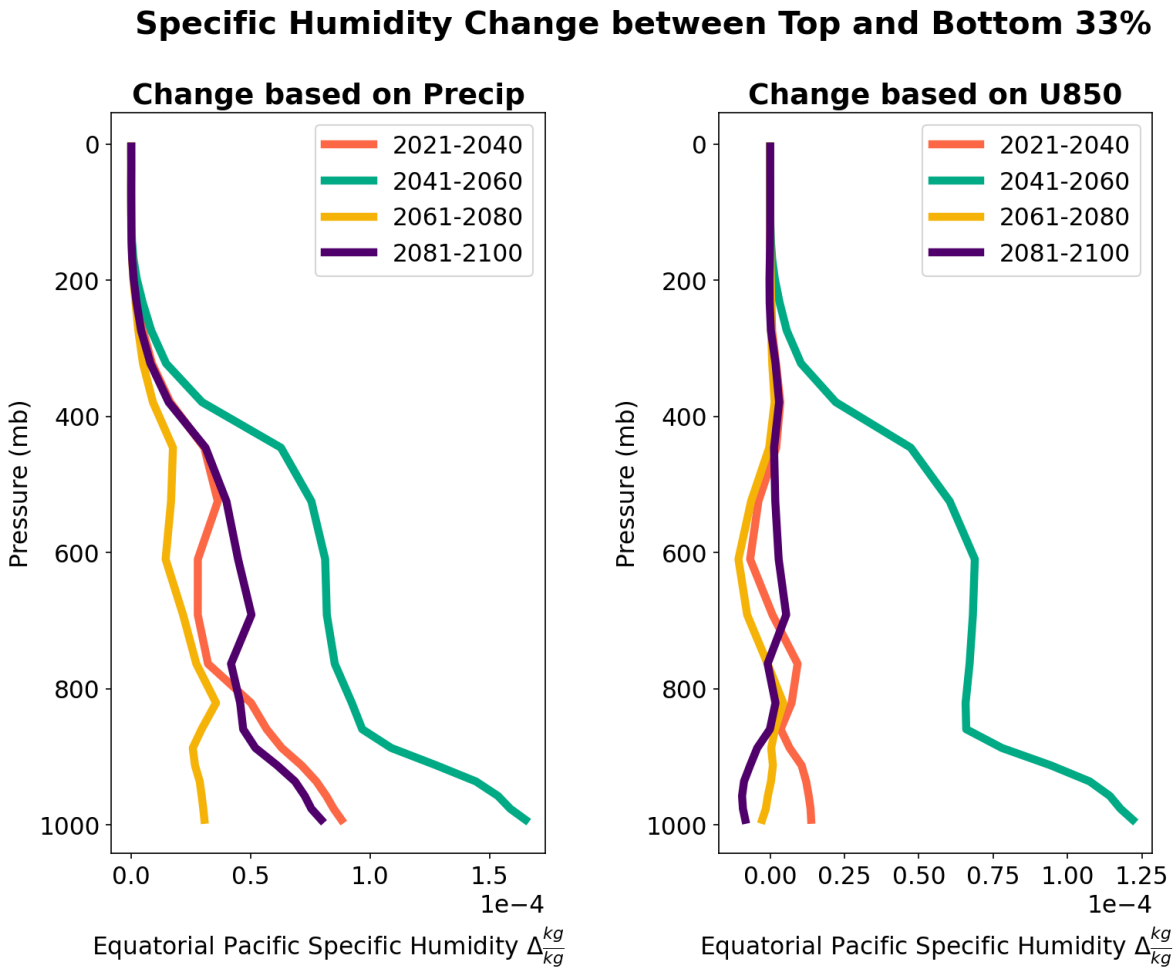

FIG. 4.5. Change of tropical Pacific vertical specific humidity profile at the Equatorial Pacific associated with the members having the top 33% minus bottom 33% of MJO amplitude changes based on precipitation and 850 mb zonal wind. Changes are defined relative to 1985 to 2005

The scatterplots across members is now examined in the relationship between lower troposphere specific humidity changes and MJO amplitude change, and the change in the gradient between middle and lower troposphere and MJO amplitude change. Figure 4.6 shows the change in MJO amplitude versus lower tropospheric Equatorial Pacific specific humidity change. The correlations for changes in MJO precipitation amplitude are significant but modest, with highest values earlier in the century (2041-2060) before a more general El Niño-like warming pattern commence for all ensemble members.

The correlations associated with zonal wind amplitude change are generally weaker and not significant in 2081-2100.

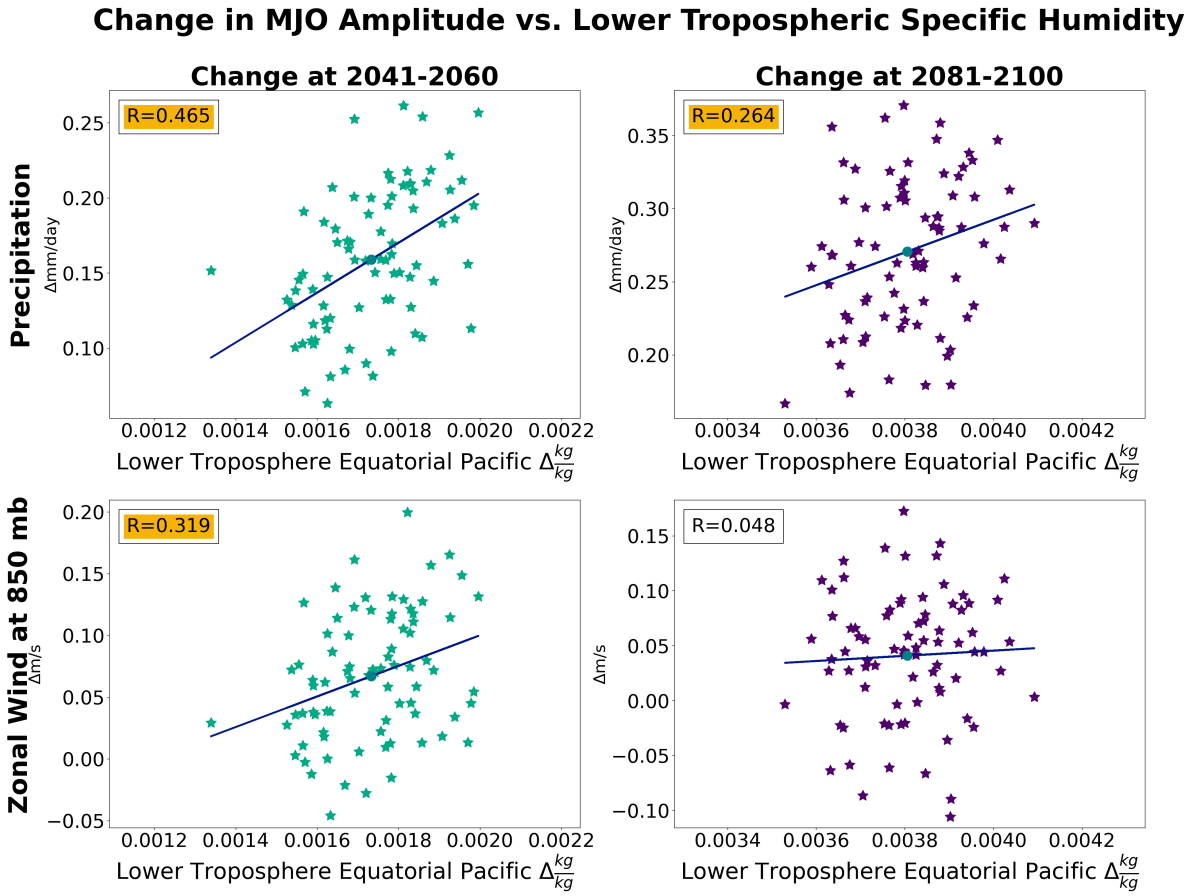

FIG. 4.6. Relationship between MJO precipitation and wind amplitude change averaged over the entire tropics and lower tropospheric specific humidity change at the Equatorial Pacific relative to 1985 to 2005 for two 20-yr periods.

How MJO amplitude change relates to changes in the vertical specific humidity gradient across ensemble members are also examined. In the comparison of MJO precipitation amplitude change against lower minus middle tropospheric specific humidity change, modest positive correlations exist that are significant only in 2041-2060 (Figure 4.7). This generally supports that ensemble members with stronger vertical humidity gradient change have bigger MJO amplitude increases, although other factors such as internal MJO variability are also important. Correlations associated with wind amplitude change are weaker and only significant in 2041-2060.

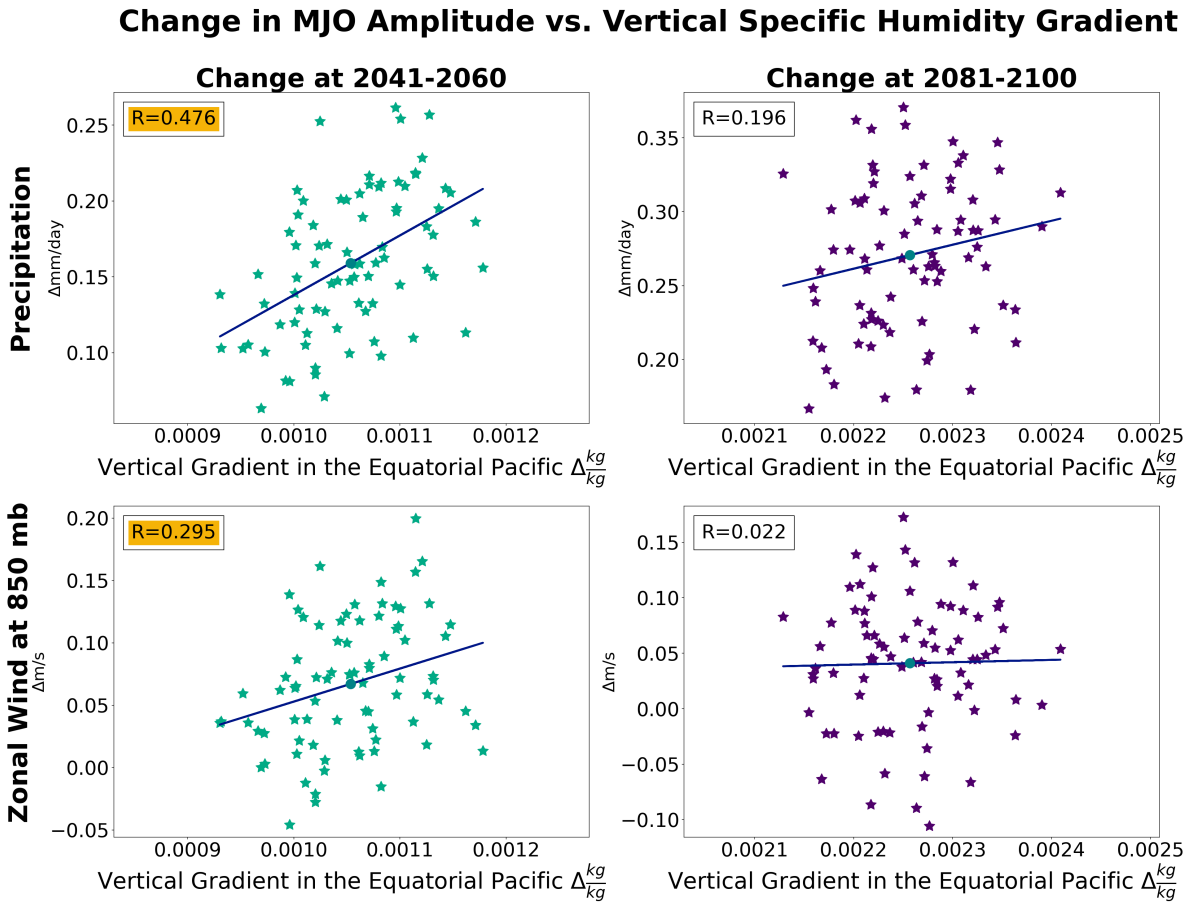

FIG. 4.7. Relationship between MJO precipitation and wind amplitude change averaged over the entire tropics and vertical specific humidity gradient change at the Equatorial Pacific relative to 1985 to 2005 for two 20-yr periods.

4.4 CONCLUSION

The analysis of projected precipitable water and the vertical moisture profiles generally shows that a moister central to eastern Pacific occurs with climate change, reflecting an El Niño-Like moistening pattern. This would generally support MJO activity viewed through the lens of moisture mode theory both by supporting MJO maintenance due to a moister lower troposphere, but also supporting MJO propagation across the Pacific through enhanced horizontal advective moistening by the MJO circulation acting across a stronger meridional moisture gradient. Why individual ensemble members have stronger MJO amplitude increases is also examined. Ensemble members with the strongest MJO precipitation amplitude increases generally have increased lower tropospheric mean vertical moisture gradients and increased meridional moisture gradients, consistent with more El Niño-like warming patterns. Substantial scatter exists in the relationship between individual ensemble members' MJO

amplitude changes and characteristics of basic state moisture changes. This likely reflects the influence of internal variability in MJO activity on the results.

CHAPTER 5

CONCLUSION

The CESM2 large ensemble under the SSP370 forcing scenario is used to assess how the pattern of SST change in a warmer climate impacts MJO amplitude. In general, the ensemble mean SST and precipitation pattern change look El Niño-like, producing ensemble mean increases in MJO precipitation and wind amplitude in the tropics, with the strongest increase in variability in the central through eastern Pacific. The ensemble mean change in MJO wind amplitude is substantially less than precipitation amplitude, consistent with increases in tropical static stability and weaker circulation magnitudes per unit diabatic heating under WTG theory. Before the midpoint of the 21st Century, individual ensemble members can have SST warming patterns substantially weighted toward the west, central, or east Pacific. Later in the century, the projected SST pattern indicate an El Niño-like central and eastern equatorial Pacific warming pattern relative to the historical period baseline with less variability between ensemble members. Ultimately, this investigation is useful because it is consistent with existing literature, but adds the aspect of warming and MJO projections over vulnerable communities. Most importantly, this investigation analyzes MJO projections through a large ensemble members spread in a same, newer model.

The investigation next examined how SST pattern change in a warmer climate between ensemble members influence the amplitude of MJO change in the tropics (Maloney and Xie 2013). Under moisture mode theory, MJO propagates eastward more prominently and maintains its amplitude longer when SST and meridional moisture gradients are increased and higher equatorial SST increases the vertical moisture gradient (Sobel and Maloney 2012, 2013). CESM2 ensemble members with the highest tropics-wide MJO precipitation amplitude increase diagnosed through the difference between MJO plus (top 33% of members) and MJO minus (bottom 33% of members) exhibit a more El Niño-Like warming pattern. The analysis of projected precipitable water and vertical moisture profiles with these high MJO amplitude members show a stronger meridional TMQ gradient, which would produce more moistening to the east of MJO convection in the central to eastern Pacific by the horizontal MJO flow through meridional moisture advection. This is reflective of a warming pattern that is more El Niño-like. The TMQ meridional gradient change is especially notable in the central Pacific for these high amplitude members. Members with greater El Niño-like warming also support an increased vertical

humidity gradient in the tropical Pacific, which would better maintain the MJO through vertical advection. The correlation of individual ensemble members' MJO precipitation amplitude change with east Pacific SST warming change, and horizontal and vertical humidity gradient changes, indicate significant, but modest, positive correlations. The 2041-2060 period tends to produce the most robust relationships between MJO amplitude and characteristics of the background environment as the climate warms. Thus, the study concludes that projected SST pattern change does influence MJO precipitation amplitude. Moreover, the investigation does support the hypothesis that moisture mode theory is effective for explaining how the MJO's maintenance and propagation changes in a warmer climate. In general, simulations with the greatest changes in MJO wind amplitude are not explained as easily by changes in the background SST state.

The impact of SST pattern change on the mean precipitation and MJO amplitude change for specific tropical islands and oceanic regions was also examined. In general, the strongest consistent island precipitation change signals occur in the eastern Pacific, with uncertainty in the pattern of SST change presumably making prediction of mean precipitation for the west and central Pacific more uncertain. The greatest MJO amplitude change favors Central Polynesia, although ensemble members still show substantial spread. These results highlight the challenges in predicting water resource availability for tropical islands in the future. Climate action through adaptation and mitigation strategies can help overcome adversity in climate change hazards given this uncertainty. Climate action can be a needed step to reduce the impact of climate change to communities through mitigation, adaptation, or geoengineering strategies. Mitigation takes proactive steps to reduce unnecessary amplification of severe climate hazards, while adaptation strategies create suitable living biotic or geoengineering methods to cohabit with climate change hazards. Pacific islands and their respective weather offices organize the Pacific ENSO Applications Center (PEAC) to forecast precipitation and sea level (Schroeder et al. 2012), which might play a role in helping the islands prepare for climate change and its impacts. The limitations to climate change preparedness for islands is rooted in financial and political governance, lack of weather education with some due to cultural beliefs, high susceptibility to economic shock, and inadequate climate data for these regions (Mycoo et al. 2022). Thus, PEAC's strategy is to foster collaborative effort to overcome these adversities, prepare for the necessary mitigation and adaptation strategies, and to improve public awareness for oceanic regions (Schroeder et al. 2012). Island climate

change preparedness ranges from coastal protection structures such as sea walls, elevated homes, improving agroforestry, reef restoration, planting native plants for beach erosion reduction, better fishing technologies and equipment, and diversifying (salt tolerant) crops (Mycoo et al. 2022).

Future work based on this investigation is to compare how the suppressed and convective phases of the MJO will change in a future climate. Work will also be conducted to relate future temperature and moisture pattern changes and their uncertainty to societal impacts in specific oceanic regions, which contain vulnerable communities. An analysis of how atmospheric rivers (ARs) and tropical cyclones (TCs) are influenced by MJO activity changes will also be conducted.

REFERENCES

Abraham, J., L. Cheng, M. E. Mann, K. Trenberth, and K. von Schuckmann, 2022: The ocean response to climate change guides both adaptation and mitigation efforts. *Atmospheric and Oceanic Science Letters*, **15 (4)**, 100 221, doi: 10.1016/j.aosl.2022.100221, URL https://www.sciencedirect.com/science/article/pii/S1674283422000964.

Adames, F. and D. Kim, 2016: The MJO as a Dispersive, Convectively Coupled Moisture Wave: Theory and Observations. *Journal of the Atmospheric Sciences*, **73 (3)**, 913–941, doi: 10.1175/JAS-D-15-0170.1, URL https://journals.ametsoc.org/view/journals/atsc/73/3/jas-d-15-0170.1.xml.

Adames, F. and E. D. Maloney, 2021: Moisture Mode Theory's Contribution to Advances in our Understanding of the Madden-Julian Oscillation and Other Tropical Disturbances. *Current Climate Change Reports*, **7 (2)**, 72–85, doi: 10.1007/s40641-021-00172-4, URL https://link.springer.com/10.1007/s40641-021-00172-4.

Adames, F. and J. M. Wallace, 2015: Three-Dimensional Structure and Evolution of the Moisture Field in the MJO. *Journal of the Atmospheric Sciences*, **72 (10)**, 3733–3754, doi: 10.1175/JAS-D-15-0003.1, URL https://journals.ametsoc.org/view/journals/atsc/72/10/jas-d-15-0003.1.xml.

Arnold, N. P., M. Branson, Z. Kuang, D. A. Randall, and E. Tziperman, 2015: MJO Intensification with Warming in the Superparameterized CESM. *Journal of Climate*, **28 (7)**, 2706–2724, doi: 10.1175/JCLI-D-14-00494.1, URL https://journals.ametsoc.org/view/journals/clim/28/7/jcli-d-14-00494.1.xml.

Bingham, C., M. Godfrey, and J. Tukey, 1967: Modern techniques of power spectrum estimation. *IEEE Transactions on Audio and Electroacoustics*, **15 (2)**, 56–66, doi: 10.1109/TAU.1967.1161895, URL http://ieeexplore.ieee.org/document/1161895/.

Bui, H. X., Y.-X. Li, E. D. Maloney, J.-E. Kim, S.-S. Lee, and J.-Y. Yu, 2023: Emergence of Madden-Julian oscillation precipitation and wind amplitude changes in a warming climate. *npj Climate and Atmospheric Science*, **6 (1)**, 1–6, doi: 10.1038/s41612-023-00344-z, URL https://www.nature.com/articles/s41612-023-00344-z.

Bui, H. X. and E. D. Maloney, 2018: Changes in Madden-Julian Oscillation Precipitation and Wind Variance Under Global Warming. *Geophysical Research Letters*, **45 (14)**, 7148–7155, doi: 10.1029/2018GL078504, URL https://onlinelibrary.wiley.com/doi/abs/10.1029/2018GL078504.

Bui, H. X. and E. D. Maloney, 2022: Changes to tropical eastern North Pacific intraseasonal variability under global warming, implications for tropical cyclogenesis. *Atmósfera*, **35 (4)**, 611–631, doi: 10.20937/ATM.53021, URL https://www.revistascca.unam.mx/atm/index.php/atm/article/view/53021.

Danabasoglu, G., et al., 2020: The Community Earth System Model Version 2 (CESM2). *Journal of Advances in Modeling Earth Systems*, **12 (2)**, e2019MS001 916, doi: 10.1029/2019MS001916, URL https://onlinelibrary.wiley.com/doi/abs/10.1029/2019MS001916.

DeMott, C. A., B. O. Wolding, E. D. Maloney, and D. A. Randall, 2018: Atmospheric Mechanisms for MJO Decay Over the Maritime Continent. *Journal of Geophysical Research: Atmospheres*, **123 (10)**, 5188–5204, doi: 10.1029/2017JD026979, URL https://onlinelibrary.wiley.com/doi/abs/10.1029/2017JD026979.

Diffenbaugh, N. S. and E. A. Barnes, 2023: Data-driven predictions of the time remaining until critical global warming thresholds are reached. *Proceedings of the National Academy of Sciences*, **120 (6)**, e2207183 120, doi: 10.1073/pnas.2207183120, URL https://www.pnas.org/doi/full/10.1073/pnas.2207183120.

Gonzalez, A. O. and X. Jiang, 2017: Winter mean lower tropospheric moisture over the Maritime Continent as a climate model diagnostic metric for the propagation of the Madden-Julian oscillation. *Geophysical Research Letters*, **44 (5)**, 2588–2596, doi: 10.1002/2016GL072430, URL https://onlinelibrary.wiley.com/doi/abs/10.1002/2016GL072430.

Gottschalck, J., 2014: What is the MJO, and why do we care? | NOAA Climate.gov. URL http://www.climate.gov/news-features/blogs/enso/what-mjo-and-why-do-we-care.

Hayashi, M. and H. Itoh, 2017: A New Mechanism of the Slow Eastward Propagation of Unstable Disturbances with Convection in the Tropics: Implications for the MJO. *Journal of the Atmospheric Sciences*, **74 (11)**, 3749–3769, doi: 10.1175/JAS-D-16-0300.1, URL https://journals.ametsoc.org/view/journals/atsc/74/11/jas-d-16-0300.1.xml.

Hsiao, W.-T., E. D. Maloney, and E. A. Barnes, 2020: Investigating Recent Changes in MJO Precipitation and Circulation in Multiple Reanalyses. *Geophysical Research Letters*, **47 (22)**, e2020GL090 139, doi: 10.1029/2020GL090139, URL https://onlinelibrary.wiley.com/doi/abs/10.1029/2020GL090139.

Huang, K., J. H. Richter, and K. V. Pegion, 2023: Captured QBO-MJO Connection in a Subseasonal Prediction System. *Geophysical Research Letters*, **50 (8)**, e2022GL102 648, doi: 10.1029/2022GL102648, URL https://onlinelibrary.wiley.com/doi/abs/10.1029/2022GL102648.

Hurrell, J. W., et al., 2013: The Community Earth System Model: A Framework for Collaborative Research. *Bulletin of the American Meteorological Society*, **94 (9)**, 1339–1360, doi: 10.1175/BAMS-D-12-00121.1, URL https://journals.ametsoc.org/view/journals/bams/94/9/bams-d-12-00121.1.xml.

Hwang, Y.-T. and D. M. W. Frierson, 2013: Link between the double-Intertropical Convergence Zone problem and cloud biases over the Southern Ocean. *Proceedings of the National Academy of Sciences*, **110 (13)**, 4935–4940, doi: 10.1073/pnas.1213302110, URL https://www.pnas.org/doi/10.1073/pnas.1213302110.

Jiang, X., et al., 2020: Fifty Years of Research on the Madden-Julian Oscillation: Recent Progress, Challenges, and Perspectives. *Journal of Geophysical Research: Atmospheres*, **125 (17)**, e2019JD030911, doi: 10.1029/2019JD030911, URL https://onlinelibrary.wiley.com/doi/abs/10.1029/2019JD030911.

Jones, C. and L. M. V. Carvalho, 2011: Will global warming modify the activity of the Madden-Julian Oscillation? *Quarterly Journal of the Royal Meteorological Society*, **137 (655)**, 544, URL https://www.academia.edu/11758552/Will_global_warming_modify_the_activity_of_the_Madden_Julian_Oscillation.

Kang, D., D. Kim, M.-S. Ahn, and S.-I. An, 2021: The Role of the Background Meridional Moisture Gradient on the Propagation of the MJO over the Maritime Continent. *Journal of Climate*, **34 (16)**, 6565–6581, doi: 10.1175/JCLI-D-20-0085.1, URL https://journals.ametsoc.org/view/journals/clim/34/16/JCLI-D-20-0085.1.xml.

Kay, J. E., et al., 2015: The Community Earth System Model (CESM) Large Ensemble Project: A Community Resource for Studying Climate Change in the Presence of Internal Climate Variability. *Bulletin of the American Meteorological Society*, **96 (8)**, 1333–1349, doi: 10.1175/BAMS-D-13-00255.1, URL https://journals.ametsoc.org/view/journals/bams/96/8/bams-d-13-00255.1.xml.

Kiladis, G. N., K. H. Straub, and P. T. Haertel, 2005: Zonal and Vertical Structure of the Madden–Julian Oscillation. *Journal of the Atmospheric Sciences*, **62 (8)**, 2790–2809, doi: 10.1175/JAS3520.1, URL https://journals.ametsoc.org/view/journals/atsc/62/8/jas3520.1.xml.

Kiladis, G. N., M. C. Wheeler, P. T. Haertel, K. H. Straub, and P. E. Roundy, 2009: Convectively coupled equatorial waves. *Reviews of Geophysics*, **47 (2)**, doi: 10.1029/2008RG000266, URL https://onlinelibrary.wiley.com/doi/abs/10.1029/2008RG000266.

Kim, D., H. Kim, and M.-I. Lee, 2017: Why does the MJO detour the Maritime Continent during austral summer? *Geophysical Research Letters*, **44 (5)**, 2579–2587, doi: 10.1002/2017GL072643, URL https://onlinelibrary.wiley.com/doi/abs/10.1002/2017GL072643.

Lee, R. W., S. J. Woolnough, A. J. Charlton-Perez, and F. Vitart, 2019: ENSO Modulation of MJO Teleconnections to the North Atlantic and Europe. *Geophysical Research Letters*, **46 (22)**, 13 535–13 545, doi: 10.1029/2019GL084683, URL https://onlinelibrary.wiley.com/doi/abs/10.1029/2019GL084683.

Lefale, P. F., 2010: Ua 'afa le Aso Stormy weather today: traditional ecological knowledge of weather and climate. The Samoa experience. *Climatic Change*, **100 (2)**, 317–335, doi: 10.1007/s10584-009-9722-z, URL https://doi.org/10.1007/s10584-009-9722-z.

Lorenz, E. N., 1963: Deterministic Nonperiodic Flow. *Journal of the Atmospheric Sciences*, **20 (2)**, 130–141, doi: 10.1175/1520-0469(1963)020<0130:DNF>2.0.CO;2, URL https://journals.ametsoc.org/view/journals/atsc/20/2/1520-0469_1963_020_0130_dnf_2_0_co_2.xml.

Madden, R. A. and P. R. Julian, 1971: Detection of a 40–50 Day Oscillation in the Zonal Wind in the Tropical Pacific. *Journal of the Atmospheric Sciences*, **28 (5)**, 702–708, doi: 10.1175/1520-0469(1971)028<0702:DOADOI>2.0.CO;2, URL https://journals.ametsoc.org/view/journals/atsc/28/5/1520-0469_1971_028_0702_doadoi_2_0_co_2.xml.

Madden, R. A. and P. R. Julian, 1972: Description of Global-Scale Circulation Cells in the Tropics with a 40–50 Day Period. *Journal of the Atmospheric Sciences*, **29 (6)**, 1109–1123, doi: 10.1175/1520-0469(1972)029<1109:DOGSCC>2.0.CO;2, URL https://journals.ametsoc.org/view/journals/atsc/29/6/1520-0469_1972_029_1109_dogscc_2_0_co_2.xml.

Madden, R. A. and P. R. Julian, 1994: Observations of the 40–50-Day Tropical Oscillation—A Review. *Monthly Weather Review*, **122 (5)**, 814–837, doi: 10.1175/1520-0493(1994)122<0814:OOTDTO>2.0.CO;2, URL https://journals.ametsoc.org/view/journals/mwre/122/5/1520-0493_1994_122_0814_ootdto_2_0_co_2.xml.

Maloney, E. D., 2009: The Moist Static Energy Budget of a Composite Tropical Intraseasonal Oscillation in a Climate Model. *Journal of Climate*, **22 (3)**, 711–729, doi: 10.1175/2008JCLI2542.1, URL https://journals.ametsoc.org/view/journals/clim/22/3/2008jcli2542.1.xml.

Maloney, E. D., F. Adames, and H. X. Bui, 2019: Madden–Julian oscillation changes under anthropogenic warming. *Nature Climate Change*, **9 (1)**, 26–33, doi: 10.1038/s41558-018-0331-6, URL https://www.nature.com/articles/s41558-018-0331-6.

Maloney, E. D. and D. L. Hartmann, 1998: Frictional Moisture Convergence in a Composite Life Cycle of the Madden–Julian Oscillation. *Journal of Climate*, **11 (9)**, 2387–2403, doi: 10.1175/1520-0442(1998)011<2387:FMCIAC>2.0.CO;2, URL https://journals.ametsoc.org/view/journals/clim/11/9/1520-0442_1998_011_2387_fmciac_2.0.co_2.xml.

Maloney, E. D. and D. L. Hartmann, 2000: Modulation of Eastern North Pacific Hurricanes by the Madden–Julian Oscillation. *Journal of Climate*, **13 (9)**, 1451–1460, doi: 10.1175/1520-0442(2000)013<1451:MOENPH>2.0.CO;2, URL https://journals.ametsoc.org/view/journals/clim/13/9/1520-0442_2000_013_1451_moenph_2.0.co_2.xml.

Maloney, E. D. and S.-P. Xie, 2013: Sensitivity of tropical intraseasonal variability to the pattern of climate warming. *Journal of Advances in Modeling Earth Systems*, **5 (1)**, 32–47, doi: 10.1029/2012MS000171, URL https://onlinelibrary.wiley.com/doi/abs/10.1029/2012MS000171.

Meehl, G. A. and W. M. Washington, 1996: El Niño-like climate change in a model with increased atmospheric CO2 concentrations. *Nature*, **382 (6586)**, 56–60, doi: 10.1038/382056a0, URL https://www.nature.com/articles/382056a0.

Mycoo, M., et al., 2022: Small Islands. In: Climate Change 2022: Impacts, Adaptation and Vulnerability. Contribution of Working Group II to the Sixth Assessment Report of the Intergovernmental Panel on Climate Change. *Cambridge University Press*, 2043–2121, doi: 10.1017/9781009325844.017.

Neelin, J. D. and I. M. Held, 1987: Modeling Tropical Convergence Based on the Moist Static Energy Budget. *Monthly Weather Review*, **115 (1)**, 3–12, doi: 10.1175/1520-0493(1987)115<0003:MTCBOT>2.0.CO;2, URL https://journals.ametsoc.org/view/journals/mwre/115/1/1520-0493_1987_115_0003_mtcbot_2_0_co_2.xml.

Raymond, D. J. and Fuchs, 2009: Moisture Modes and the Madden–Julian Oscillation. *Journal of Climate*, **22 (11)**, 3031–3046, doi: 10.1175/2008JCLI2739.1, URL https://journals.ametsoc.org/view/journals/clim/22/11/2008jcli2739.1.xml.

Riahi, K., et al., 2017: The Shared Socioeconomic Pathways and their energy, land use, and greenhouse gas emissions implications: An overview. *Global Environmental Change*, **42**, 153–168, doi: 10.1016/j.gloenvcha.2016.05.009, URL https://www.sciencedirect.com/science/article/pii/S0959378016300681.

Richter, I. and T. Doi, 2019: Estimating the Role of SST in Atmospheric Surface Wind Variability over the Tropical Atlantic and Pacific. *Journal of Climate*, **32 (13)**, 3899–3915, doi: 10.1175/JCLI-D-18-0468.1, URL https://journals.ametsoc.org/view/journals/clim/32/13/jcli-d-18-0468.1.xml.

Rodgers, K. B., et al., 2021: Ubiquity of human-induced changes in climate variability. *Earth System Dynamics*, **12 (4)**, 1393–1411, doi: 10.5194/esd-12-1393-2021, URL https://esd.copernicus.org/articles/12/1393/2021/.

Rugenstein, M., et al., 2020: Equilibrium Climate Sensitivity Estimated by Equilibrating Climate Models. *Geophysical Research Letters*, **47 (4)**, e2019GL083 898, doi: 10.1029/2019GL083898, URL https://onlinelibrary.wiley.com/doi/abs/10.1029/2019GL083898.

Schroeder, T. A., M. R. Chowdhury, M. A. Lander, C. C. Guard, C. Felkley, and D. Gifford, 2012: The Role of the Pacific ENSO Applications Climate Center in Reducing Vulnerability to Climate Hazards: Experience from the U.S.-Affiliated Pacific Islands. *Bulletin of the American Meteorological Society*, **93 (7)**, 1003–1015, doi: 10.1175/BAMS-D-11-00109.1, URL https://journals.ametsoc.org/view/journals/bams/93/7/bams-d-11-00109.1.xml.

Sobel, A. and E. Maloney, 2012: An Idealized Semi-Empirical Framework for Modeling the Madden–Julian Oscillation. *Journal of the Atmospheric Sciences*, **69 (5)**, 1691–1705, doi: 10.1175/JAS-D-11-0118.1, URL https://journals.ametsoc.org/view/journals/atsc/69/5/jas-d-11-0118.1.xml.

Sobel, A. and E. Maloney, 2013: Moisture Modes and the Eastward Propagation of the MJO. *Journal of the Atmospheric Sciences*, **70 (1)**, 187–192, doi: 10.1175/JAS-D-12-0189.1, URL https://journals.ametsoc.org/view/journals/atsc/70/1/jas-d-12-0189.1.xml.

Sobel, A. H. and C. S. Bretherton, 2000: Modeling Tropical Precipitation in a Single Column. *Journal of Climate*, **13 (24)**, 4378–4392, doi: 10.1175/1520-0442(2000)013<4378:MTPIAS>2.0.CO;2, URL http://journals.ametsoc.org/doi/10.1175/1520-0442(2000)013<4378:MTPIAS>2.0.CO;2.

Takahashi, C., N. Sato, A. Seiki, K. Yoneyama, and R. Shirooka, 2011: Projected Future Change of MJO and its Extratropical Teleconnection in East Asia during the Northern Winter Simulated in IPCC AR4 Models. *SOLA*, **7**, 201–204, doi: 10.2151/sola.2011-051, URL http://www.jstage.jst.go.jp/article/sola/7/0/7_0_201/_article.

Tompkins, A. M., 2001: On the Relationship between Tropical Convection and Sea Surface Temperature. *Journal of Climate*, **14 (5)**, 633–637, doi: 10.1175/1520-0442(2001)014<0633:OTRBTC>2.0.CO;2, URL https://journals.ametsoc.org/view/journals/clim/14/5/1520-0442_2001_014_0633_otrbtc_2.0.co_2.xml.

Trenberth, K. E., 1997: The Definition of El Niño. *Bulletin of the American Meteorological Society*, **78 (12)**, 2771–2778, doi: 10.1175/1520-0477(1997)078<2771:TDOENO>2.0.CO;2, URL https://journals.ametsoc.org/view/journals/bams/78/12/1520-0477_1997_078_2771_tdoeno_2_0_co_2.xml.

Trenberth, K. E., G. W. Branstator, D. Karoly, A. Kumar, N.-C. Lau, and C. Ropelewski, 1998: Progress during TOGA in understanding and modeling global teleconnections associated with tropical sea surface temperatures. *Journal of Geophysical Research: Oceans*, **103 (C7)**, 14 291–14 324, doi: 10.1029/97JC01444, URL https://onlinelibrary.wiley.com/doi/abs/10.1029/97JC01444.

Waliser, D. E., 1996: Formation and Limiting Mechanisms for Very High Sea Surface Temperature: Linking the Dynamics and the Thermodynamics. *Journal of Climate*, **9 (1)**, 161–188, doi: 10.1175/1520-0442(1996)009<0161:FALMFV>2.0.CO;2, URL https://journals.ametsoc.org/view/journals/clim/9/1/1520-0442_1996_009_0161_falmfv_2_0_co_2.xml.

Wheeler, M. and G. N. Kiladis, 1999: Convectively Coupled Equatorial Waves: Analysis of Clouds and Temperature in the Wavenumber–Frequency Domain. *Journal of the Atmospheric Sciences*, **56 (3)**, 374–399, doi: 10.1175/1520-0469(1999)056<0374:CCEWAO>2.0.CO;2, URL https://journals.ametsoc.org/view/journals/atsc/56/3/1520-0469_1999_056_0374_ccewao_2.0.co_2.xml.

Wheeler, M. C. and H. H. Hendon, 2004: An All-Season Real-Time Multivariate MJO Index: Development of an Index for Monitoring and Prediction. *Monthly Weather Review*, **132 (8)**, 1917–1932, doi: 10.1175/1520-0493(2004)132<1917:AARMMI>2.0.CO;2, URL https://journals.ametsoc.org/view/journals/mwre/132/8/1520-0493_2004_132_1917_aarmmi_2.0.co_2.xml.

Xie, S.-P., C. Deser, G. A. Vecchi, J. Ma, H. Teng, and A. T. Wittenberg, 2010: Global Warming Pattern Formation: Sea Surface Temperature and Rainfall. *Journal of Climate*, **23 (4)**, 966–986, doi: 10.1175/2009JCLI3329.1, URL https://journals.ametsoc.org/view/journals/clim/23/4/2009jcli3329.1.xml.

Yang, S., Z. Li, J.-Y. Yu, X. Hu, W. Dong, and S. He, 2018: El Niño–Southern Oscillation and its impact in the changing climate. *National Science Review*, **5 (6)**, 840–857, doi: 10.1093/nsr/nwy046, URL https://doi.org/10.1093/nsr/nwy046.

Yeo, M.-H., J. Pangelinan, and R. King, 2022: Identifying Characteristics of Guam's Extreme Rainfalls Prior to Climate Change Assessment. *Water*, **14 (10)**, 1578, doi: 10.3390/w14101578, URL https://www.mdpi.com/2073-4441/14/10/1578.

Zhou, Y., H. Kim, and D. E. Waliser, 2021: Atmospheric River Lifecycle Responses to the Madden-Julian Oscillation. *Geophysical Research Letters,* **48 (3)**, e2020GL090 983, doi: 10.1029/2020GL090983, URL https://onlinelibrary.wiley.com/doi/abs/10.1029/2020GL090983.

APPENDIX

FREQUENCY-WAVENUMBER MJO AMPLITUDE TOOL

The precipitation and zonal wind at 850 mb is detrended by least squared regression fit. The frequency-wavenumber domain bandpass shows a strong MJO signal for 30-90 days frequency, 1-5 zonal wavenumber (k) (Wheeler and Kiladis 1999). MJO signals in precipitation and 850 mb zonal wind are isolated by a bandpass filter for this region of the frequency-wavenumber domain (Bingham et al. 1967). The mathematical framework to perform filtering techniques and pattern changes. This filtering is composed of several scripts written in Python. The code with pathfiles and environmental variables can be changed to adapt to the user's needs. These scripts for filtering and MJO analysis is publicly available on Github: https://github.com/Mandy453?tab=repositories.

The first script uses NCAR CESM2 LENS surface temperature and precipitation are used.

- Input Files
  - Global 1.25° x 0.94° TS (Surface temperature (radiative)) and PRECT (Total (convective and large-scale) precipitation rate (liq+ice))
- Output Files
  - NCAR CESM2 LENS PRECT.nc
  - NCAR CESM2 LENS TS.nc
- Objective
  (1) Crop the data in the Boreal Winter Period as well as different 20-yr decadal period.
  (2) Calculate mean change for TS and Precipitation.
  (3) Calculate Pacific oceanic regions and their associated islands for 20-yr decadal period
  (4) Calculate Pacific oceanic regions and their associated islands

The second script performs Fourier frequency-wavenumber bandpass filtering (also known as kf filter) of a variable in time made by Jared Rennie. NCAR CESM2 LENS surface PRECT, OLR, and U850 (zonal wind at 850 mb) are used.

- Input Files
  - Global 1.25° x 0.94° PRECT, OLR, and U850
- Output Files
  - NCAR CESM2 LENS PRECT.nc
  - NCAR CESM2 LENS OLR.nc
  - NCAR CESM2 LENS U850.nc
- Objective
  (1) Fourier filtering of PRECT, OLR, and U850 in time

The third script performs Fourier filtering referenced from Jared Rennie (see second script). NCAR CESM2 LENS surface PRECT, OLR, and U850 (zonal wind at 850 mb) are used. NCAR CESM2 LENS surface temperature on a monthly period is used.

- Input Files
  - Global 1.25° x 0.94° PRECT, OLR, TS, and U850
- Output Files
  - NCAR CESM2 LENS PRECT.nc
  - NCAR CESM2 LENS OLR.nc
  - NCAR CESM2 LENS U850.nc
  - NCAR CESM2 LENS TS.nc
- Objective
  (1) Crop the data in the Boreal Winter Period as well as different 20-yr decadal period.
  (2) Calculate mean change for PRECT and U850.
  (3) Calculate MJO Activity influence in Pacific oceanic regions for 20-yr decadal period
  (4) Calculate the top 33% and bottom 33% of the MJO amplitude through TS

The fourth script performs Fourier filtering referenced from Jared Rennie (see second script). NCAR CESM2 LENS surface PRECT, OLR, and U850 (zonal wind at 850 mb) are used. NCAR CESM2 LENS TMQ (precipitable water) and specific humidity (SHQ) on a monthly period is used.

- Input Files

  - Global 1.25° x 0.94° PRECT, OLR, SHQ, TMQ, and U850

- Output Files
  - NCAR CESM2 LENS PRECT.nc
  - NCAR CESM2 LENS OLR.nc
  - NCAR CESM2 LENS U850.nc
  - NCAR CESM2 LENS TMQ.nc
  - NCAR CESM2 LENS SHQ.nc

- Objective

(1) Crop the data in the Boreal Winter Period as well as different 20-yr decadal period.

(2) Calculate MJO Activity influence in Pacific oceanic regions for 20-yr decadal period

(3) Calculate the top 33% and bottom 33% of the MJO amplitude through TMQ

(4) Calculate the top 33% and bottom 33% of the MJO amplitude through meridional TMQ gradient

(5) Calculate the top 33% and bottom 33% of the MJO amplitude through Vertical SHQ profile

(6) Evaluate Vertical SHQ profile for the lower troposphere and lower minus middle troposphere gradient compared to MJO Activity